





METHOD ARTICLE

A miRNA screen procedure identifies *garz* as an essential factor in adult glia functions and validates *Drosophila* as a beneficial 3Rs model to study glial functions and GBF1 biology [version 1; peer review: 2 approved]

Catarina Gonçalves-Pimentel^{1,2}, David Mazaud ¹, Benjamin Kottler¹, Sandra Proelss¹, Frank Hirth¹, Manolis Fanto ^{1,3}

¹Department of Basic and Clinical Neuroscience, King's College London, London, SE5 9NU, UK

²Champalimaud Research, Champalimaud Foundation, Av. Brasília, Lisbon, 1400-038, Portugal

³Institut du Cerveau et de la Moelle épinière (ICM), 47, bd de l'hôpital, Paris, F-75013, France

v1 First published: 01 May 2020, 9:317
<https://doi.org/10.12688/f1000research.23154.1>
 Latest published: 01 May 2020, 9:317
<https://doi.org/10.12688/f1000research.23154.1>

Abstract



Invertebrate glia performs most of the key functions controlled by mammalian glia in the nervous system and provides an ideal model for genetic studies of glial functions. To study the influence of adult glial cells in ageing we have performed a genetic screen in *Drosophila* using a collection of transgenic lines providing conditional expression of micro-RNAs (miRNAs). Here, we describe a methodological algorithm to identify and rank genes that are candidate to be targeted by miRNAs that shorten lifespan when expressed in adult glia. We have used four different databases for miRNA target prediction in *Drosophila* but find little agreement between them, overall. However, top candidate gene analysis shows potential to identify essential genes involved in adult glial functions. One example from our top candidates' analysis is *gartenzweig* (*garz*). We establish that *garz* is necessary in many glial cell types, that it affects motor behaviour and, at the sub-cellular level, is responsible for defects in cellular membranes, autophagy and mitochondria quality control. We also verify the remarkable conservation of functions between *garz* and its mammalian orthologue, GBF1, validating the use of *Drosophila* as an alternative 3Rs-beneficial model to knock-out mice for studying the biology of GBF1, potentially involved in human neurodegenerative diseases.

Keywords

miRNA, glia, *Drosophila*, screens, GBF1

Open Peer Review

Reviewer Status  

	Invited Reviewers	
	1	2
version 1 01 May 2020	 report	 report

- 1 **Ivana Bjedov**, University College London, London, UK
- 2 **Jeff W. Barclay**, University of Liverpool, Liverpool, UK

Any reports and responses or comments on the article can be found at the end of the article.



This article is included in the NC3Rs gateway.

Corresponding author: Manolis Fanto (manolis.fanto@kcl.ac.uk)

Author roles: **Gonçalves-Pimentel C:** Data Curation, Investigation, Methodology, Writing – Original Draft Preparation; **Mazaud D:** Data Curation, Investigation, Methodology, Writing – Review & Editing; **Kottler B:** Data Curation, Methodology, Writing – Review & Editing; **Proelss S:** Data Curation, Investigation; **Hirth F:** Funding Acquisition, Supervision; **Fanto M:** Conceptualization, Data Curation, Funding Acquisition, Resources, Supervision, Writing – Original Draft Preparation, Writing – Review & Editing

Competing interests: B.K. is co-founder of BFK Lab LTD

Grant information: This work was supported by grants from the NC3Rs (NC/L000199/1) and the Ataxia UK (2491) awarded to M.F. and by grants from the MRC (MR/L010666/1) and the BBSRC (BB/N001230/1) to F.H.

The funders had no role in study design, data collection and analysis, decision to publish, or preparation of the manuscript.

Copyright: © 2020 Gonçalves-Pimentel C *et al.* This is an open access article distributed under the terms of the [Creative Commons Attribution License](#), which permits unrestricted use, distribution, and reproduction in any medium, provided the original work is properly cited.

How to cite this article: Gonçalves-Pimentel C, Mazaud D, Kottler B *et al.* **A miRNA screen procedure identifies *garz* as an essential factor in adult glia functions and validates *Drosophila* as a beneficial 3Rs model to study glial functions and GBF1 biology [version 1; peer review: 2 approved]** F1000Research 2020, 9:317 <https://doi.org/10.12688/f1000research.23154.1>

First published: 01 May 2020, 9:317 <https://doi.org/10.12688/f1000research.23154.1>

Research highlights

Scientific benefits:

- This screen has provided a thorough analysis of glial functions in ageing
- Potential to shortcut gene discovery through miRNAs effect. The screening of only ~200 mutant lines potentially targets >6000 genes.
- Potential to identify complex regulatory networks that include miRNAs and target genes.
- Validated the identification of essential genes for the adult nervous system and their functions specifically in motor control.
- An open-access searchable database for future discoveries upon improved precision of miRNA-target predictions.

3Rs benefits:

- This screening method provides an alternative approach for studying genes important in glial biology, without the need for animal experiments.
- Example validation that *Drosophila* can be used to study the biology of GBF1, instead of *in vivo* vertebrate animal models, such as zebrafish or mouse.

Practical benefits:

- The searchable database can be easily updated upon emergence of updated miRNA target predictions.
- RNAi lines are publicly available from the Vienna Drosophila Resource Centre stock collection.
- Genetic studies in *Drosophila* are quicker and more sophisticated compared to vertebrate studies. They also maintain high conservation of functions.

Current applications:

- Uncovered the function of *garz* in glial cells for membrane trafficking, autophagy and mitochondria quality control.
- Study of genes, such as GBF1, involved in ageing and neurodegeneration

Future applications:

- Identification of novel miRNA targets in glia
- Study of novel miRNA targets in glia
- Study of glial functions in controlling lifespan and healthspan

Introduction

Despite the fact that glial cells were initially identified simply as the connective tissue of the brain¹, work developed in the past decades has shed a light on a much more intricate role for these cells in developing and maintaining nervous system homeostasis (reviewed in 2). From neuronal nutrient supply³, to neurotransmitter recycling⁴⁻⁶, to being the first line of immune response in the brain⁷, glial cells have been shown to actively contribute to the correct functioning of the brain.

More recently, several studies have been taking advantage of *Drosophila*'s powerful genetic manipulation to better understand the role of glia in the development and maintenance of the nervous system (see 8 for review).

The use of invertebrate models is also a powerful 3Rs solution to reduce and replace animal experiments. It expressly applies to complex matters in which cross-talk between different cell types (e.g. glia and neurons) is a focal point of the investigation, given that these complex environments are more difficult to model *in vitro* and *in silico*. Popular animal models for studying glial functions are zebrafish, which provide a useful platform for tissue and cell biology, with some capability for genetic manipulation⁹ and genetically modified mice¹⁰. Despite having a different developmental origin, glial cells have converged in *Drosophila* and mammals towards the same key functions of neurotransmission regulation, insulation and immune surveillance/phagocytosis⁸, making the fruit-fly an organism of choice for studying the function of glial cells.

We have tackled the functions of glial cells in ageing. We have previously screened a large collection of miRNAs regarding their effects on *Drosophila*'s lifespan upon ectopic expression in glial cells in adult flies and have validated this screen through the analysis of *repo*, an already-established key glia gene¹¹. The experimental advantage of performing a miRNA-based screen followed by *in silico* identification and ranking of predicted miRNAs target transcripts^{11,12} has, however, its bottleneck in the validation of the action of the genes of interest. In principle, the specific knockdown of predicted target genes should mimic, to some extent, the phenotype obtained upon corresponding miRNA overexpression.

In fact, using databases of predicted miRNA-target genes previously allowed us to identify *repo* as an important player for maintaining glial function and, consequently, homeostasis in the adult brain¹¹. We have shown that while the *miR-1-repo* axis is physiologically relevant only in the embryo during the glia versus haemocyte cell fate choice¹³, the miRNA-target relationship can be exploited as a discovery tool to identify the functions of a target gene in a different context, namely adult glial functions¹¹.

While the focus on *repo* was based on its already-established role in glia cell function, here we attempt a global and unbiased systematic *in silico* approach. In order to systematically identify potential target genes that could account for the lifespan phenotype, focusing on the miRNAs that shortened lifespan, we set out to devise a quantitative algorithm. The aim of this algorithm is to identify and rank the predicted target genes so that those ranking on top would be the most relevant for adult glia in lifespan and ageing.

This is followed by experimental validation of the function of these targets in adult glia in the same paradigm used in the miRNAs screen.

We conclude that this approach is valid but has issues of efficiency given the large number of predicted targets that do not recapitulate the expected phenotype. We also establish that there is no significant synergy generated by focusing on the common predictions between all available miRNAs target databases. Nevertheless, the main outcome of our work is a list of

candidate genes whose function is essential in glial cells during ageing. These genes can be studied in the future in *Drosophila*, with the tools identified here, rather than in genetically modified mouse models or in zebrafish, providing an incentive towards animal replacement and reduction and advancing the 3Rs. Mouse and zebrafish neuroscientists and geneticists could take advantage of this information to test preliminary approaches and exploratory experiments in *Drosophila*, prior to validation in their system reducing the number of animals used. Alternatively, they may entirely replace vertebrate animals with *Drosophila* to study highly conserved genes and glial functions.

The success of this *in silico* approach is exemplified by our analysis of one of the top predicted targets: *gartenzweig* (*garz*), the fly orthologue of GBF1 (golgi brefeldin A resistant guanine nucleotide exchange factor 1), a small GTPase guanine exchange factor. Here, we show that *garz* is an essential factor in glia homeostasis maintenance.

Small GTPases regulate a wide range of cellular events such as proliferation, morphology, nuclear transport and vesicle formation¹⁴. The conversion from GDP-bound (inactive) to GTP-bound (active) forms of these enzymes relies on the activity of GTPase activating proteins (GAPs) and guanine nucleotide exchange factors (GEFs). While GAPs are responsible for their inactivation through GTP hydrolysis, GEFs are responsible for their activation promoting the exchange of GDP by GTP¹⁵.

GEFs belonging to the Sec7 domain protein family are responsible for the activation of Arf (ADP-ribosylation factor) GTPases which are associated with the recruitment of coat proteins (COP) to vesicle budding sites¹⁶⁻¹⁸. GBF1 is part of this family¹⁹ and is highly conserved in all eukaryotes, conferring significant translatability of the findings obtained using different model organisms.

Strongly localized in the cis-Golgi compartment, GBF1 has been shown to regulate vesicle trafficking between the endoplasmic reticulum (ER) and the Golgi apparatus²⁰⁻²⁴. Mutated versions or knock-down of *garz* expression brings about epithelial morphogenesis defects during development conditioning embryonic trachea and larval salivary gland formation^{30,21}. Additionally, in accordance with a role in membrane delivery and vesicular trafficking, silencing of *garz* in these glands impairs membrane delivery of adhesion molecules²⁵. Independently from its role in secretion, GBF1/*garz* has also been implicated in pinocytosis²⁶; intestinal stem cell survival²⁷; cell cycle^{28,29}; unfolded protein response events²⁹; mitochondria morphology and function³⁰; and autophagy^{31,32}.

Here we show that *garz* knock-down resulted not only in lifespan reduction but also in motor deficits of adult flies and in subcellular phenotypes indicative of dysfunctions in trafficking, autophagy and mitochondria. Additionally, miRNAs overexpression and *garz* knockdown phenotypes were reverted by expression of its mammalian orthologue GBF1, stressing the conservation of functions and the appropriateness of using

Drosophila in place of vertebrate models to study the biology of GBF1.

Methods

Online resources and in silico algorithms for target identification and ranking

The following databases were used for the prediction of miRNA targets:

- MicroCosm (<https://www.ebi.ac.uk/enright-srv/microcosm/htdocs/targets/v5/>)
- microRNA.org (<http://www.microrna.org/microrna/home.do>)
- TargetScan (http://www.targetscan.org/fly_72/)
- PicTar (<https://pictar.mdc-berlin.de/>)

Each of the databases provides for every miRNA a numerical prediction of the likelihood of targeting a given gene (Score). For MicroCosm and PicTar this was used without additional steps. In the case of miRNA.org this score is a negative value and we have squared it to obtain a positive number. In the case of TargetScan a numerical score was calculated on the basis of the information provided by the database as follows: conserved 8mer = 10 points, conserved 7mer-m8 = 6 points, conserved 7mer-1A = 4 points, poorly conserved 8mer = 8 points, poorly conserved 7mer-m8 = 4 points and poorly conserved 7mer-1A = 2 points. A detailed explanation of the 8mer and 7mer species can be found on the TargetScan website and in the original publication³³.

The algorithm for ranking targets within each database consists of two steps.

- Step 1 - column $(\text{Score}) \cdot \text{Av}(\chi^2)$ or $(\text{Score}^2) \cdot \text{Av}(\chi^2)$:
For each miRNA, every target score (or its square value) was multiplied by the Average Chi square (χ^2) obtained in the miRNAs screen (from Table 1). Information regarding different mRNAs for the same gene, where available, was grouped under the same gene name
- Step 2 - column $\Sigma(\text{Score}) \cdot \text{Av}(\chi^2)$ or $\Sigma(\text{Score}^2) \cdot \text{Av}(\chi^2)$:
For each target gene, as defined by its CG number/accession ID, all values resulting from all miRNAs predicted to target the same gene were summed in a final ranking value. Information regarding different mRNAs from the same gene, where available, was grouped under the same gene name.

The algorithm for comparing the ranking between different databases and providing a final common ranking consists of two steps:

- Step1 - column Normalised $\Sigma[(\text{Score}) \cdot \text{Av}(\chi^2)]$ or Normalised $\Sigma[(\text{Score}^2) \cdot \text{Av}(\chi^2)]$

For each database the $\Sigma(\text{Score}) \cdot \text{Av}(\chi^2)$ was normalised to 100 and then weighted for the fraction of miRNAs present in the database, out of the total tested in our miRNAs screen. For TargetScan the groups of miRNAs families were counted as one unit in each case.

Table 1. Average strength of miRNAs that shorten lifespan in adult glia. To determine the strength of miRNAs in our lifespan assay we have used the averaged χ^2 values from each transgenic line used in our previously published analysis¹¹. When only one line was tested for a given miRNA, the value was divided in half, i.e. assuming a neutral value of 0 for a second putative untested line. For the TargetScan database, some miRNAs are grouped in families requiring an amendment to our approach. In this case, we have averaged all miRNAs in the given families. Additionally, some of the lines tested for these grouped miRNAs had, in the original screen the opposite effect of what is here considered, i.e. extending lifespan with respect to the control used. To account for this opposite effect the χ^2 values for these miRNAs have been given negative values and have been effectively subtracted, when calculating the $Av(\chi^2)$ parameter.

miRNAs	$Av(\chi^2)$	$Av(\chi^2)$ Targetscan
1	44.2375	
3	55.0050	23.8583 (3 + 309 + 318)
8	11.8700	
9a	94.4800	
9b	106.5150	
9c	67.4800	89.4917 (9a + 9b + 9c)
10	5.8250	
12	22.2150	
31	1.7233	
34	61.6733	
79	75.6650	
92a	95.6050	
92b	28.3000	72.245 (92a + 92b + 310 + 312+ 313)
124	82.5700	
133	48.0200	
137	42.7400	
184	27.4050	
193	47.5300	
219	2.1550	
263b	5.5650	
274	22.6400	
276b	41.4350	25.02 (276a + 276b)
277	24.5850	
278	77.6300	
279	13.5000	-4.104 (279 + 286 + 996)
287	2.2550	
310	102.4833	
312	32.8850	72.245 (92a + 92b + 310 + 312+ 313)
313	50.7100	
315	24.5900	
316	2.6950	

miRNAs	$Av(\chi^2)$	$Av(\chi^2)$ Targetscan
318	26.3850	
375	39.2500	
932	25.8700	
958	25.4200	
968	35.0700	
977	4.7065	
978	70.4600	
980	31.0400	
989	44.3800	
992	7.8050	
995	7.0500	2.695 (285 + 995 + 998)
999	2.7750	
1015	3.8550	

- Step 2 – column $\Sigma\{\text{Normalised } \Sigma[(\text{Score}^{(2)}) * Av(\chi^2)]\}$
For each target gene, all values from all databases were summed into a final ranking number.

Drosophila stocks and husbandry

Flies were kept on standard cornmeal agar food (0.8% w/v agar, 2% w/v cornmeal, 8% w/v glucose, 5% w/v Brewer’s yeast, 1.5% v/v ethanol, 0.22% v/v methyl- 4-hydroxybenzoate, 0.38% v/v propionic acid) at 18°C or room temperature. Unless stated otherwise, *w¹¹¹⁸* flies were used as control. The following lines were acquired from the Bloomington collection: *w¹¹¹⁸* (RRID:BDSC_3605), *repo-Gal4* (RRID:BDSC_7415), *NP2222-Gal4* (RRID:DGGR_112830), *moody-Gal4*, *elav-Gal4* (RRID:BDSC_8765), *tub-Gal80^s* (RRID:BDSC_7019). *alrm-Gal4* (RRID:BDSC_67031) was kindly provided by M. Freeman (University of Massachusetts) ; *UAS-miR-1*, *UAS-miR-79* and *UAS-miR-315* were generated by E. Lai (Sloan Kettering Institute) for the miR library³⁴; *UAS-garz-RNAi* (42140/GD and 42141/GD) as well as all RNAi lines used are from Vienna *Drosophila* Resource Center (VDRC); *gliotactin-Gal4* was provided by R. Sousa-Nunes; *UAS-mito-GFP* was provided by J. Bateman; *UAS-garz*; *UAS-garz^{Sec7-}*; *UAS-GBF1* and *UAS-ΔGBF1^{Sec7-}* were kindly provided by S. Luschnig.

Lifespan

Lifespan analysis was performed as previously described³⁵. Briefly, crosses were maintained at 18°C throughout the whole development of the progeny. Within the first 5 days post-eclosion, adult flies were collected, and female and male flies pooled together. An equal number of flies was distributed in three vials, a total of 60 flies was used. This group size has a power of 0.8 in one tailed survival test at 50% survival for the control group and 29% for an experimental group at 0.05 significance. Lifespan assessment was performed in a controlled environment

of 29°C and 60% humidity, three times a week. Upon short CO₂ anaesthesia (5 s), the number of dead vs alive flies was counted, and the alive flies transferred into a fresh vial.

Motor behaviour assay

Single fly tracking was carried out as previously described¹¹. In each experiment, up to 20 flies per genotype were placed into individual glass tubes. This group size has a power of 0.9 and significance 0.05 for three groups with an effect size of 0.48, as measured for the mean bout length. All the genotypes were positioned on the same platform, having two shaft-less motors placed underneath each subplatform containing each, one genotype. The protocol used consisted of 6 stimuli events equally split during a period of 2 h and 15 min, the first one starting after 30 min of recording and the last one 30 min before the end of the protocol. Each stimuli event was composed of 5 vibrations of 200 ms spaced by 500 ms. The x/y position of each single fly was tracked and analysed using DART software 1.0 (freely distributed upon request to info@bfklab.com) in order to evaluate the relative speed and activity before, during and after the stimuli event. The speed analysis was used for the “Stimuli Response Trace” and the general activity used to deduce “Active Speed”, “Mean Bout Length” and “Inter-Bout Interval”, using a custom-made modification of the DART software³⁶. Raw data were analysed with GraphPad Prism for statistical significance and DART-derived graphs were edited with Adobe Illustrator CC2017 (RRID:SCR_010279).

Immunostaining

Flies (N=5–10) were briefly (5 s) anesthetized with CO₂ and kept on ice, entire fly brains were dissected under a stereoscope and immediately fixed in 4% paraformaldehyde (PFA, from EMS) in Phosphate Buffer Saline (PBS) for 30 min. After washing with PBS, the brains were incubated for blocking in PBS with 0.3% triton-X (BDH 306324N) (PBT) and 10% foetal bovine serum (Sigma F4135) for 1 hr. Primary antibody incubation was done overnight at 4°C and followed by three washes (20 min each) in PBT. Secondary antibody incubation for 1hr at room temperature was followed by three washes. All steps were in 50- μ l volume in a 96-well plate on a gentle rocker. Brains were then mounted on a slide in Vectashield with DAPI (Vector Labs). The following primary antibodies, diluted in blocking solution (see above): anti-Repo (1/100, mouse DSHB 8D12, RRID:AB_528448); anti-GFP (1/1000, rabbit, Life technologies, A11122) anti-GFP(1/100, mouse, Roche, RRID: AB_390913), anti-GFP (1/500, chicken, kindly provided by M. Meyer); anti-Ref(2)P (1/2000, rabbit, a gift of Tor Erik Rusten). Secondary antibodies were all from Life technologies (conjugated with Alexa-488, Alexa-555 or Alexa-666) and diluted 1/200 in blocking solution (see above).

Z-stacks at intervals of 0.3 μ m or 5 μ m were taken at 1024 \times 1024 pixel/inch resolution. For control vs *garz^{IR}* comparisons, microscope settings were established using control flies to have a GFP signal below saturation and kept unchanged throughout all acquisitions. All images were acquired with a Leica TCS SP5 confocal microscope and mitochondria sphericity, volume and surface area in [Figure 3B,C](#) were

measured using the [3D Object Counter 2.0.1](#) plugin³⁷ in the [ImageJ Fiji 1.52n](#) software (RRID:SCR_002285).

Statistical analysis

All statistical analysis was performed with Graph-Pad Prism 7 software (RRID:SCR_002798). For all lifespans, the statistical analysis was performed using the log-rank test of the Kaplan and Meier method. For behavioural experiments (DART), the statistical analysis was done by one-way ANOVA using Dunnett’s multiple comparisons post hoc test. Significance is shown by asterisks in all figures as follows: *P<0.05, **P<0.01, ***P<0.001, and ****P<0.0001.

Randomization and blinding

In each experiment the desired number of flies were selected haphazardly from a much larger cohort of flies with the same genotype and sex. Blinding was performed in lifespan and behaviour by masking the genotypes with a numerical or alphabetical serial labelling.

Results

Development of an algorithm for ranking miRNA target genes for their relevance in adult glia in lifespan and ageing

Firstly, such algorithm should prioritise the information for the miRNAs that had the strongest effect on the fly lifespan in our miRNA screen. To achieve this, we have quantified the average strength of each miRNA using the Chi square (χ^2) of each Kaplan Mayer analysis ([Table 1](#)).

To identify potential target genes, we used four different databases available online: EBI MicroCosm, PicTar, microRNA.org and TargetScan. Each database weights the likelihood of every miRNA to target a given gene with a numerical score. Where this is different, for TargetScan, we calculated a numerical score on the basis of the sequence information provided by the database (see *Methods*).

Therefore, to rank target genes within each database taking into account both the likelihood of being targeted by a given miRNA and the strength of the effect of this miRNA in adult glia, we first multiplied the average strength of each miRNA from our screen (values in [Table 1](#)) by the strength of the target prediction (Score) given by the database, obtaining the parameter (Score)*Av(χ^2). This was done for all miRNAs tested in our screen that were present in each database.

Because a given gene can be targeted by more than one miRNA, to rank its overall importance in adult glia, we have summed all the values obtained for a given gene that were calculated for different miRNAs, obtaining the parameter $\Sigma[(\text{Score}) * \text{Av}(\chi^2)]$. In the case of TargetScan, some miRNAs are grouped in families and we have considered them as a single unit value. This underweights these miRNAs in comparison to others and the genes targeted by them (for instance a gene targeted by miR-9a, miR-9b and miR-9c would obtain a $\Sigma[(\text{Score}) * \text{Av}(\chi^2)]$ that is the sum of three (Score)*Av(χ^2) in the other databases, but for TargetScan it would only reflect one (Score)*Av(χ^2). Our reasoning was that grouped miRNAs in TargetScan was not taking

into account valuable information and this should be reflected in a penalisation in the ranking.

In conclusion we have ranked target genes according to $\Sigma[(\text{Score}) * \text{Av}(\chi^2)]$ for EBI MicroCosm (Extended data Table 1)³⁸, PicTar (Extended data Table 2)³⁸, microRNA.org (Extended data Table 3)³⁸ and TargetScan (Extended data Table 4)³⁸. Surprisingly, this revealed that there was very little agreement among the four databases. The top-ranking genes obtained using the same algorithm were very different and only 5.6% (i.e. 520 genes) of target predictions were common to all four databases (Figure 1A).

To rank these common targets for their predicted overall relevance in adult glia in ageing, we have devised additional steps. First, to make the numerical rankings from each database comparable, we have calculated the Normalised $\Sigma[(\text{Score}) * \text{Av}(\chi^2)]$ parameter by normalising the maximum value to 100. Additionally, we have weighted this number for the fraction of miRNAs present in each database, out of the total tested in our miRNAs screen. Out of 44 miRNAs screened, 31 were present in EBI MicroCosm, 28 in PicTar, 43 in microRNA.org and 40 in TargetScan. The rationale for this weighting was to prioritise the databases carrying more information that was relevant to our screen. Then, for each target gene, we have combined all these scores from the four databases generating the final parameter $\Sigma\{\text{Normalised } \Sigma[(\text{Score}^{(2)}) * \text{Av}(\chi^2)]\}$ for all targets, including the 520 that were commonly predicted by all databases (Table 2).

Systematic experimental testing of the prediction, ranking and effectiveness of different databases

To test these predictions, we decided to screen for the lifespan effect, a number of RNAi lines from Vienna *Drosophila* Resource Center (VDRC) that were already present in our stock collection. These corresponded to a random selection of approximately 10% (51 out of 520) of commonly predicted target genes. Adopting a similar strategy used for the miRNA screen, we have used the *repo-Gal4*, *tub-Gal80^s* inducible system to trigger the RNAi expression in all glial cells in adult flies. As negative control, we used the offspring of crossing *repo-Gal4*, *tub-Gal80^s* to *w¹¹¹⁸* throughout the screen. The expectation was that RNAi against these target genes in adult glia, would phenocopy the effect of the miRNAs that are predicted to target them, therefore shortening lifespan.

The gold standard commonly used by the *Drosophila* community to gain confidence about the effects of RNAi knock-down is to obtain a similar effect when testing two RNAi lines against the same gene (2-RNAi lines criterion). Remarkably, only in six cases at least two different RNAi lines tested for the same gene delivered the shorter lifespan phenotype that was predicted (Table 3). In another case both RNAi lines tested had the same effect, but it was the opposite of the predicted one, extending lifespan with respect to the control flies.

In other cases (11/51) there was an overall confirmation of the prediction, but the two RNAi lines tested for one given target did

not share the same effect or we were able to test only one line. The largest group (19/51) was made by cases in which there was no effect and surprisingly in a remarkable number of cases (14/51) there was an overall effect opposite to that predicted, albeit either the two RNAi lines tested for one given target did not share the same effect or we were able to test only one line.

In addition to the 2-RNAi lines criterion we have devised a quantitative index for ranking these targets by combining their effect in the RNAi screen (averaging the Chi square for the RNAi lines targeting each gene, $\text{Av}(\chi^2)\text{IR}$) with the strength of the prediction in all combined databases ($\Sigma\{\text{Normalised } \Sigma[(\text{Score}) * \text{Av}(\chi^2)]\}$).

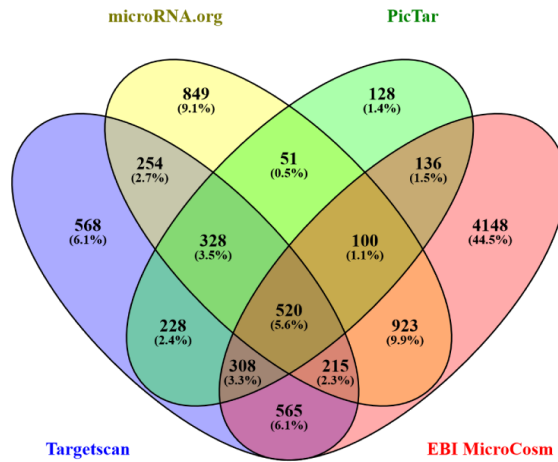
This parameter ($\Sigma\{\text{Normalised } \Sigma[(\text{Score}) * \text{Av}(\chi^2)]\} * \{\text{Av}(\chi^2)\text{IR}\}$) highlighted *garz*, one of the six targets satisfying the 2-RNAi lines criterion, as the top target (Table 3). However, there was incomplete agreement with respect to the rest of the ranking between the two criteria, i.e. our scoring system and the rule of 2-RNAi lines, with only four of the ten top scores coming from target genes satisfying the 2-RNAi lines criterion.

We also tested 14 additional targets that were differentially predicted by the different databases. We were able to further identify five targets that confirmed the predicted phenotype, one satisfying also the 2-RNAi lines criterion, while two had the opposite overall effect (Table 4).

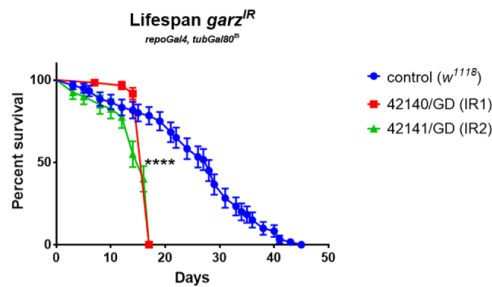
A comparison between these two groups, the common to all databases and the differentially predicted, highlights that the fraction of validated prediction is similar, but the chance of finding false positives (i.e. targets that had the opposite effect to that predicted) is paradoxically higher in the commonly predicted group (15/51 in the common and 2/14 in the differential).

Considering the lack of tangible benefits of focusing on the commonalities between the different databases, we have then exploited our validation analysis to quantify the prediction capability of each of the four databases to identify the most valid for our screen. For all targets tested, both from the common group (Table 3) and from the differential group (Table 4), we have calculated the database-specific Normalised $\Sigma[(\text{Score}) * \text{Av}(\chi^2)] * \{\text{Av}(\chi^2)\text{IR}\}$ parameter by combining the quantification of the lifespan effect of the RNAi lines (average Chi square in the RNAi screen) with the normalised predicted score from each database. Then, to rank databases we have summed all these results (with a negative value for false positives) to determine the predicting power score. TargetScan had the highest predicting power for the list of common targets, while MicroCosm had the highest capacity for target identification among the differential targets. PicTar had the lowest predicting power in all cases. However, MicroCosm also predicted the largest number of genes as targets of our miRNA screen, with over 44% of them not shared by the other databases. We reasoned that this lack of efficiency in EBI MicroCosm had to be considered and when normalising for the total number of predicted targets from each database, as a measure of the predicting power efficiency, TargetScan showed a greater efficiency in both cases, followed by miRNA.org.

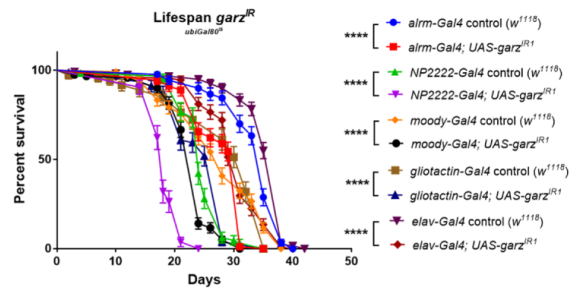
A



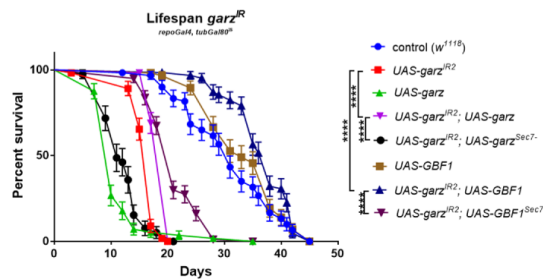
B



C



D



E

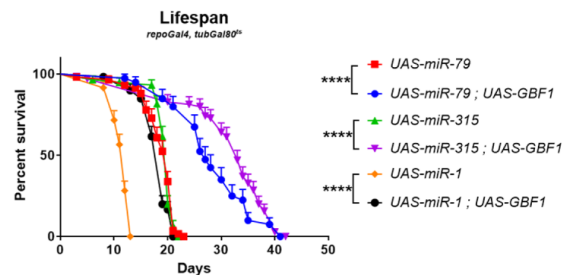


Figure 1. Effects of *garz* knock-down in adult glial cell. (A) Venn diagram referring to the data in Table 6 and illustrating the overlap between the four different databases used to predict gene targets of the miRNAs whose expression in the adult glia resulted in a significant reduction in fly lifespan. Only 520 target genes are in common among all four databases, *garz* falls in this group. A remarkably large number of genes as targets were uniquely predicted by the MicroCosm database. **(B)** Two RNAi lines against *garz* bring about a very significant reduction in fly lifespan in comparison to controls, when expressed in all adult glia. N=60 for each genotype, Error bars SEM, pairwise comparisons: Log-rank (Mantel-Cox) test. The full dataset can be accessed at DOI [10.17605/OSF.IO/8E3NS](https://doi.org/10.17605/OSF.IO/8E3NS) as part of Table 7. **(C)** Knock-down of *garz* in sub-populations of glial cells, astrocyte-like (*alrm-Gal4*), Cortex glia (*NP2222-Gal4*), sub-perineural glia (*moody-Gal4*), perineural and PNS glia (*gliotactin-gal4*) or in neurons (*elav-Gal4*) brings about a significant reduction in lifespan in comparison to controls. N=60 for each genotype, Error bars SEM, pairwise comparisons: Log-rank (Mantel-Cox) test. The full dataset can be accessed at DOI [10.17605/OSF.IO/HQCDG](https://doi.org/10.17605/OSF.IO/HQCDG). **(D)** Lifespan reduction due to RNAi against *garz* in adult glia is rescued by an exogenous *UAS-garz* transgene and by a transgene expressing the human orthologue GBF1 under *UAS* control. Note that overexpression of *garz* in an otherwise wt background is highly detrimental to fly lifespan, whereas overexpression of GBF1 in a wt background has no adverse effects. Mutations leading to a non-functional Sec7 domain eliminate or drastically reduce the ability of *garz* or *GBF1* transgenes to rescue fly lifespan. N=60 for each genotype, Error bars SEM, pairwise comparisons: Log-rank (Mantel-Cox) test. The full dataset can be accessed at DOI [10.17605/OSF.IO/5RGEF](https://doi.org/10.17605/OSF.IO/5RGEF). **(E)** Co-expression of human GBF1 significantly extends the short lifespan caused by overexpression of miR-1, miR-79 and miR-315 in adult glia. N=60 for each genotype, Error bars SEM, pairwise comparisons: Log-rank (Mantel-Cox) test. The full dataset can be accessed at DOI [10.17605/OSF.IO/B37DF](https://doi.org/10.17605/OSF.IO/B37DF).

Table 2. Identification and ranking of target predictions common to all four databases. The ranking scores from all four databases were pooled to obtain a global rank of all targets predicted by our analysis and a list of targets that are predicted by all four databases. Because the different databases contained information about some, but not all, miRNAs analysed in our screen we have weighted the completeness of each database by normalising the $\Sigma[(\text{Score}) \cdot \text{Av}(\chi^2)]$ by the fraction of miRNAs listed in the database, out of the ones tested in our screen. In addition, to make the ranking from each database equally valued in this analysis, we have normalised each score to 100 as a maximum possible value for each database – column Normalised $\Sigma[(\text{Score}) \cdot \text{Av}(\chi^2)]$. Thereafter, all values for each target have been added – column $\Sigma\{\text{Normalised } \Sigma[(\text{Score}) \cdot \text{Av}(\chi^2)]\}$ – for each target and for a specific list of 520 targets that have been predicted by all four databases, albeit with different scores. Only the top 30 rows are shown here. The full table can be accessed at <https://doi.org/10.17605/OSF.IO/QWUJAY>.

Pooled Non Redundant			520 Common elements in “Targetscan”, “microRNA.org”, “PicTar” and “EBI MicroCosm”:		
GENE NAME	CG No	$\Sigma\{\text{Normalised } \Sigma[(\text{Score}^{(2)}) \cdot \text{Av}(\chi^2)]\}$	GENE NAME	CG No	$\Sigma\{\text{Normalised } \Sigma[(\text{Score}^{(2)}) \cdot \text{Av}(\chi^2)]\}$
CG7852	CG7852	206.8084	CG7852	CG7852	206.8084
CrebA	CG7450	165.9009	CadN	CG7100	148.5861
CadN	CG7100	148.5861	nerfin-1	CG13906	129.7977
sha	CG13209	133.6386	Cpr50Ca	CG13338	125.1063
CG31191	CG31191	130.1998	Nak	CG10637	103.4518
nerfin-1	CG13906	129.7977	CG11206	CG11206	95.6901
CG13338	CG13338	125.1063	CG8128	CG8128	94.2880
CG4297	CG4297	122.1155	up	CG7107	94.0563
Mef2	CG1429	113.9984	CG3077	CG3077	0.0000
Khc-73	CG8183	110.5961	porin	CG6647	89.8516
A2bp1	CG32062	108.8272	CG14015	CG14015	89.2605
Nak	CG10637	103.4518	CG33090	CG33090	82.8792
Rbp9	CG3151	102.6802	ttk	CG1856	81.3790
CG11206	CG11206	95.6901	Sbf	CG6939	73.9455
sinu	CG10624	94.9798	Klp68D	CG7293	72.5983
CG8128	CG8128	94.2880	CG12024	CG12024	72.3875
up	CG7107	94.0563	CG10737	CG10737	71.3749
w	CG5123	91.9243	rau	CG8965	70.9517
CG3077	CG3077	91.2297	CG9426	CG9426	69.5509
porin	CG6647	89.8516	salm	CG6464	68.5351
CG14015	CG14015	89.2605	Thd1	CG1981	66.7116
CG14274	CG14274	87.6812	Dysb	CG6856	65.1018
Eip93F	CG18389	84.3128	rho	CG1004	64.6470
CG33090	CG33090	82.8792	Vha68-1	CG12403	64.4111
lola	CG12052	81.8661	CG8323	CG8323	64.1433
ttk	CG1856	81.3790	CG4853	CG4853	63.3083
srp	CG3992	81.2668	CG9650	CG9650	62.1572
ck	CG7595	80.9393	SP555	CG14041	61.7540
CG32767	CG32767	78.9667	CdsA	CG7962	61.6698
sdk	CG5227	74.9601	RhoGAP68F	CG6811	61.4035
Sbf	CG6939	73.9455	Opa1	CG8479	61.2329

Table 3. Match between experimental RNAi and predictions for targets common to all databases. Strength of the effect on fly lifespan of RNAi lines against some of the gene targets predicted by all four databases. For most genes two different RNAi lines have been tested. In red are the lines that, in agreement with the miRNA prediction, shorten the lifespan, in comparison to controls (w1118) when specifically expressed in the adult flies with repo-Gal4 and tub-Gal80ts. In green are the lines that have the opposite effect and prolong lifespan. In black are the lines that had no effect. Highlighted in yellow are the genes for which all lines tested had the same effect and shortened lifespan. Highlighted in pink is the gene for which all lines tested had the same effect and prolonged the lifespan. To combine the target RNAi strength with the strength of the prediction we have averaged the χ^2 for each miRNA according to the same rules followed in Table 1 and multiplied it for the final score from Table 2 – column $\Sigma[(\text{Normalised } \Sigma[(\text{Score})^2 \cdot \text{Av}(\chi^2)] \cdot \text{Av}(\chi^2))] \cdot \text{Av}(\chi^2)]$. The top rank was achieved by garz, which was also one of the 6 genes with all RNAi lines tested having the same effect. We have also repeated the same procedure separately for the four different databases using the final normalised score (Normalised $\Sigma[(\text{Score})^2 \cdot \text{Av}(\chi^2)]$) obtained from each database in Tables 2, 3, 4 and 5, and also reported in Table 2 – columns Normalised $\Sigma[(\text{Score})^2 \cdot \text{Av}(\chi^2)] \cdot \text{Av}(\chi^2)]$ for each database. The predicting power for the combination of all databases and for each database sums all scores in this column to quantify the global predicting value of each database in comparison to their combination. This is further normalised by the number of predicted targets for the whole screen, to measure the efficiency of each database when predicting target genes. The full dataset can be accessed at DOI [10.17605/OSF.IO/8E3NS](https://doi.org/10.17605/OSF.IO/8E3NS).

Target	Lines	Median survival	χ^2	Common to all databases				EBI MicroCoem		PicTar		microRNA.org		Targetscan	
				p-values	Av(χ^2)	β (Normalised $\frac{\beta[(\text{Score})^2 \cdot \text{Av}(\chi^2)]}{\text{Av}(\chi^2)}}$)	Normalised $\frac{\beta[(\text{Score})^2 \cdot \text{Av}(\chi^2)]}{\beta[(\text{Score})^2 \cdot \text{Av}(\chi^2)]}$	Normalised $\frac{\beta[(\text{Score})^2 \cdot \text{Av}(\chi^2)]}{\beta[(\text{Score})^2 \cdot \text{Av}(\chi^2)]}$	Normalised $\frac{\beta[(\text{Score})^2 \cdot \text{Av}(\chi^2)]}{\beta[(\text{Score})^2 \cdot \text{Av}(\chi^2)]}$	Normalised $\frac{\beta[(\text{Score})^2 \cdot \text{Av}(\chi^2)]}{\beta[(\text{Score})^2 \cdot \text{Av}(\chi^2)]}$	Normalised $\frac{\beta[(\text{Score})^2 \cdot \text{Av}(\chi^2)]}{\beta[(\text{Score})^2 \cdot \text{Av}(\chi^2)]}$	Normalised $\frac{\beta[(\text{Score})^2 \cdot \text{Av}(\chi^2)]}{\beta[(\text{Score})^2 \cdot \text{Av}(\chi^2)]}$	Normalised $\frac{\beta[(\text{Score})^2 \cdot \text{Av}(\chi^2)]}{\beta[(\text{Score})^2 \cdot \text{Av}(\chi^2)]}$	Normalised $\frac{\beta[(\text{Score})^2 \cdot \text{Av}(\chi^2)]}{\beta[(\text{Score})^2 \cdot \text{Av}(\chi^2)]}$	
Blimp-1	108374KK	27	3.9090	0.0480											
	34976GD	33	0.3226	0.5700	49.9482	105.6603	15.8908	33.6217	3.4973	7.3986	14.1885	29.9777	16.3916	34.6813	
Bx	106496KK	24	4.1666	0.0412											
	2971GD	27	7.2880	0.0069	59.9239	337.4571	12.5711	71.9346	10.0509	57.5614	21.5938	123.6680	14.7081	84.2331	
Cudn	101644KK	31	0.0939	0.7593											
	1092GD	31	4.3900	0.0361	-2.1481	-319.1725	20.0306	-43.0271	46.4332	-98.7416	38.4779	-82.6531	43.6443	-93.7507	
CG10737	106833KK	32	0.1800	0.6714											
	8996GD	19	36.3400	<0.0001	18.2600	1303.3054	35.5040	648.3023	5.7587	105.1168	13.7227	250.5759	16.3916	299.9104	
CG11206	42943GD	35	8.4800	<0.0001											
	42945GD	28	0.9996	0.3174	-3.7402	-357.9003	9.0084	-35.6533	8.5247	-31.8840	34.9136	-130.5659	43.2434	-16.17391	
CG12918	105503KK	35	10.6800	0.0011											
	38092GD	31	0.0029	0.9573	-5.3436	-278.5678	20.8109	-111.2046	3.3907	-18.1183	16.0949	-96.6912	9.8350	-52.5538	
CG13806	109897KK	31	3.1620	0.0754											
	45481GD	29	0.0578	0.81	1.6099	84.7431	14.5549	23.4320	4.7616	7.6658	16.6199	26.7566	16.7020	26.8887	
CG3077	109618KK	31	3.1620	0.0754											
	25630GD	29	0.0404	0.8301	1.6012	146.0771	23.2887	37.2898	6.4559	10.3372	41.8153	66.9546	19.6699	31.4955	
CG32105	108747KK	28	2.5090	0.1132											
	51267GD	28.5	2.6060	0.1064	2.5570	110.7687	10.3112	26.3658	2.2363	5.7182	20.9373	53.5367	9.8350	25.1480	
CG33090	23407GD	29	0.5904	0.4423											
	28033GD	28	0.1904	0.6626	0.3904	62.8792	21.1135	8.2427	4.0624	1.5859	16.7976	6.5578	40.9057	15.9696	
CG3376	12226GD	29	0.3743	0.5406	0.1872	42.0182	8.9405	1.5609	5.9978	1.1225	17.8450	3.3397	9.8350	1.8406	
	109666KK	35	8.7280	0.0031											
CG3534	41276GD	30	0.7	0.9995	-4.3640	-212.3199	17.7977	-77.6690	3.4824	-15.1971	17.5376	-76.5341	9.8350	-42.9197	
	36304GD	27	0.4244	0.5148											
CG3824	956GD	26	5.9420	0.0148	3.1632	176.5522	16.9653	54.0040	2.6852	8.5476	23.3858	74.4417	12.4274	39.5589	
	105000KK	25	2.6370	0.1044											
CG4360	26520GD	25	6.9190	0.0085	4.7780	228.9108	18.0506	86.2459	2.4584	11.7464	11.0087	52.5996	16.3916	78.3190	
	10057GD	31	0.4919	0.4831											
CG4894	107854KK	33	6.4300	0.0112	-2.9891	-176.5827	18.0490	-53.5884	7.6279	-22.6477	7.6745	-22.7861	26.1230	-77.5605	
	106456KK	29	0.9585	0.3276											
CG5599	16505GD	18	44.3800	<0.0001	22.6593	919.5590	8.8509	200.5549	1.0127	22.9470	12.8686	291.5939	17.8498	404.4632	
	11017KK	23	12.2400	0.0005											
CG6129	22094GD	21	15.9900	<0.0001	14.1150	41.6798	6.8082	98.0981	2.8427	40.1250	14.9821	211.4727	17.0467	240.6141	
	105468KK	31	1.4210	0.2333											
CG7510	8352GD	24	12.4400	0.0004	6.9305	49.2790	14.8554	102.9554	2.4046	16.6851	12.5453	86.9454	19.4736	134.9621	
	105666KK	33	5.6770	0.0172	-0.7240	-39.2289	7.7300	-5.5965	2.9878	-2.1632	8.4767	-6.1371	34.9891	-25.3321	
CG8121	10754KK	31	0.0685	0.7936											
	97740GD	34.5	16.3700	<0.0001	-8.1508	-768.5205	19.9651	-162.7308	3.0917	-25.1994	54.8397	-446.9861	16.3916	-133.6042	

Target	Lines	Median survival	χ^2	p-values	Common to all databases					EBI MicroCosm			PicTur			microRNA.org			Targetscan					
					Av(β /R)	β (Normalised β /(Score) β /R)	Normalised β /(Score) β /R	Normalised β /(Score) β /R	Normalised β /(Score) β /R	Normalised β /(Score) β /R	Normalised β /(Score) β /R	Normalised β /(Score) β /R	Normalised β /(Score) β /R	Normalised β /(Score) β /R	Normalised β /(Score) β /R	Normalised β /(Score) β /R	Normalised β /(Score) β /R	Normalised β /(Score) β /R	Normalised β /(Score) β /R	Normalised β /(Score) β /R	Normalised β /(Score) β /R			
CG5333	10710/KK 4918/GD	26 25	7.9890 14.6800	0.0096 0.0001	11.0345 49.7826	549.3362 174.4940	15.8126 18.4807	3.3083 4.3704	36.5052 7.7968	14.2702 13.6601	157.4640 24.3696	16.3916 27.6321	180.8730 49.2957											
CG8323	4861/GD	29	3.5660	0.0589	1.7840	114.4316	16.8753	4.3704	7.7968	11.2122	28.9484	22.9482	55.1561											
CG8360	23461/GD	34	4.8070	0.0283	-2.4035	-136.4185	16.8753	5.7226	-13.7542															
CG8417	106461/KK	38	23.1700	<0.0001																				
CG8509/GD	48529/GD	31	0.0690	0.9244	-11.5805	-606.9652	15.8653	4.3959	-50.9072	15.9226	-164.5075	16.3916	-169.8227											
CG9376	106962/KK	34	20.1300	<0.0001	-10.0650	-159.8522	7.2495	0.5563	-5.5966	3.1890	-32.0968	4.8872	-49.1895											
CG9650	104402/KK	33	0.8672	0.3517																				
CG9650	23170/GD	29	2.53E-05	0.996	0.4336	26.9522	7.6917	3.3352	7.0478	23.3065	10.1060	24.1113	10.4549											
Cpr	107422/KK	38	31.0800	<0.0001	-15.5400	-738.2286	14.3186	9.1431	-142.0838	14.2084	-220.7964	9.8950	-152.8352											
Dysb	106957/KK	32	1.6390	0.2005																				
Dysb	34354/GD	29	0.1023	0.7491																				
Dysb	34355/GD	34	3.3460	0.0674	1.6958	65.1018	19.4330	32.9539	4.5585	20.0348	33.9743	21.0755	35.7391											
endoB	104712/KK	38	39.1400	<0.0001																				
Eto1L	42140/GD	17	42.4800	<0.0001																				
gear	42141/GD	16	48.2800	<0.0001																				
Glat2	17187/GD	27	1.0330	0.3094	0.9978	41.9768	15.8440	3.1358	3.1287	13.1641	13.1345	9.8950	9.8128											
Myd88	25402/GD	28	2.0360	0.1515	1.9035	6.4706	4.1638	7.9256	0.0231	2.0501	3.9023	0.2446	0.4656											
Nek	109507/KK	29	0.4342	0.5098																				
Nek	35482/GD	29	0.0124	0.9112	0.2233	103.4518	19.0669	4.2579	3.6612	36.5532	8.1629	31.4370	7.0203											
pdm2	102126/KK	31	2.1180	0.1455	1.0590	25.7957	6.5096	0.9607	1.0173	4.8823	5.1704	13.4431	14.2362											
potm	101336/KK	38	15.4000	<0.0001	-7.7000	89.8516	62.5375	-481.5385	-19.4065	2.9915	-23.0343	21.8023	-167.8776											
Rhp6D	27091/GD	27	2.4770	0.1155																				
Rhp6D	40631/GD	29	0.3666	0.5432	1.4233	52.3718	14.2880	20.3361	6.8889	19.0121	27.0599	12.1828	17.3398											
RASSF8	105823/KK	31	0.9831	0.3214																				
RASSF8	26520/GD	27	0.8016	0.3706	0.8924	34.0327	4.4412	3.9631	0.7073	8.3362	7.4388	20.5480	18.3360											
raw	101255/KK	35	17.5900	<0.0001																				
raw	24532/GD	14	38.8600	<0.0001	10.6850	43.2677	11.3523	120.7318	65.0234	15.1605	161.4449	10.9028	115.9513											
regucalcin	105509/KK	31	1.0220	0.312																				
regucalcin	39945/GD	22	18.7500	<0.0001	9.8860	56.0884	15.5743	153.9677	155.7325	14.9263	147.5610	9.8950	97.2283											
RhoGAP6F	10775/KK	28	3.0870	0.0789																				
RhoGAP6F	34520/GD	31	0.0767	0.7818	1.5819	61.4035	14.2428	22.5303	2.8817	19.0121	30.0747	26.3289	41.6457											
Sbf	22317/GD	35	8.9180	0.0028	-4.4590	73.9455	-329.7229	28.9461	-129.0661	4.3431	-19.3659	23.8515	-105.4621											
sens	106029/KK	34	7.399	0.0065	-3.6895	49.4627	-182.9672	14.7634	-54.6171	2.6482	-9.7972	23.1217	-65.5388											
Shi2	103790/KK	30	5.7360	0.0166																				
Shi2	21989/GD	31	4.0000	0.0455	-4.8680	44.5940	-216.7917	15.6316	-76.0947	13.7227	-68.8020	9.8950	-47.8766											
SP555	39821/GD	19	19.5700	<0.0001	9.7850	61.7540	20.8951	204.4589	76.4074	17.9622	175.7604	15.0880	147.6358											
T48	100334/KK	11	21.3000	<0.0001																				
T48	100339/KK	11	21.3000	<0.0001																				
Tmd1	110439/KK	29	0.7217	0.3956	0.3609	66.7116	24.0729	19.9882	2.1996	24.2192	8.7395	20.3047	7.3289											
Tm1	34119/GD	19	10.7400	0.001	5.3700	37.4083	200.8623	9.7291	52.2401	3.4708	18.6380	14.5862	78.3281											
Uee	107892/KK	23	15.4400	<0.0001																				
Uee	46515/GD	27	10.7400	0.001	13.9900	47.8611	17.7450	232.2915	42.5476	17.0908	222.9338	9.8950	128.7395											
up	27853/GD	25	7.8600	0.0051	3.9300	94.0563	32.8545	129.1183	96.7114	24.4104	95.9330	12.1828	47.8784											
Vha68-1	17102/GD	28	0.7032	0.4017																				
Vha68-1	46397/GD	28	0.5468	0.4596	0.6250	64.4111	40.2570	9.5403	3.4957	26.8446	16.7779	24.5305	15.3316											
Predicting power					4843.1509					1178.4057					1284.1503					2100.6298				
Predicting power normalised for number of targets predicted					0.3227					0.1704					0.3902					0.6990				

Table 4. Match between experimental RNAi and predictions for targets not in common to all databases. Strength of the effect on fly lifespan of RNAi lines against some of the gene targets predicted by some, but not all, databases. In red are the lines that, in agreement with the miRNA prediction, shorten the lifespan, in comparison to controls (w1118) when specifically expressed in the adult flies with repo-Gal4 and tub-Gal80ts. In green are the lines that have the opposite effect and prolong lifespan. In black are the lines that had no effect. Highlighted in yellow is the gene for which all lines tested had the same effect and shortened lifespan. To combine the target RNAi strength with the strength of the prediction we have averaged the χ^2 for each miRNA according to the same rules followed in Table 1 and multiplied it for the final normalised score (Normalised $\Sigma[(\text{Score})^* \text{Av}(\chi^2)]$) obtained from each database in Extended data Tables 1, 2, 3 and 4 [49], and also reported in Table 2 – columns Normalised $\Sigma[(\text{Score})^* \text{Av}(\chi^2)]$ * $[\text{Av}(\chi^2)]/R$ for each database. The predicting power for each database sums all scores in this column to quantify the global predicting value of each database. This is further normalised by the number of predicted targets for the whole screen, to measure the efficiency of each database when predicting target genes, as in Table 3. The full dataset can be accessed at DOI [10.17605/OSF.IO/Q7ASN](https://doi.org/10.17605/OSF.IO/Q7ASN).

Target	Lines	Median survival	χ^2	p-values	Av(χ^2)/R	EBI MicroCosm		PicTar		microRNA.org		Targetscan	
						Normalised $\Sigma[(\text{Score})^* \text{Av}(\chi^2)]$	Normalised $\Sigma[(\text{Score})^* \text{Av}(\chi^2)]$	Normalised $\Sigma[(\text{Score})^* \text{Av}(\chi^2)]$	Normalised $\Sigma[(\text{Score})^* \text{Av}(\chi^2)]$	Normalised $\Sigma[(\text{Score})^* \text{Av}(\chi^2)]$	Normalised $\Sigma[(\text{Score})^* \text{Av}(\chi^2)]$	Normalised $\Sigma[(\text{Score})^* \text{Av}(\chi^2)]$	Normalised $\Sigma[(\text{Score})^* \text{Av}(\chi^2)]$
CG15544	39997/GD	28	0.2505	0.6167	0.1253	1.2446	0.1559	0.0137	0.0017		0.1564	0.0196	
CG1623	107655/KK	26	3.0500	0.0808									
	32665/GD	27	2.8150	0.0934	2.9325	14.6090	42.8407			20.3535	13.6183	39.9357	
CG17712	105119/KK	31	0.3146	0.5749									
	32987/GD	26	8.8560	0.0029	4.5853	16.4402	75.3831			12.5865	9.8350	45.0962	
CG3678	26267/GD	22	35.9900	<0.0001									
	49793/GD	24	13.3600	0.0003	24.6750	22.2661	549.4160			15.6470	9.8350	242.6775	
CG4893	110188/KK	31	1.0850	0.2977									
	22336/GD	26	10.6800	0.0011	5.8825	19.6009	115.3024			21.6375	20.3047	119.4422	
fray	101058/KK	38	22.8600	<0.0001									
	27944/GD	31	0.2749	0.6001	-11.2926						1.0625	-11.9986	
Ggamma1	28894/GD	32.5	3.4180	0.0645	1.7090			10.0845	17.2344	3.4702	18.7955	32.1215	
	102194/KK	33	0.2422	0.6226	0.1211	0.0986	0.0119			10.2664			
Nek2	103408/KK	33	0.6786	0.4101									
	40052/GD	26	5.5540	0.0184	3.1163	29.1504	90.8415			13.6972	9.8350	30.6487	
nord	39901/GD	31	0.0068	0.9341	0.0034			0.0120	0.0000	3.5694	0.3669	0.0013	
Paf-A-Haloha	101683/KK	33	6.2970	0.0121	-3.1485	2.4176	-7.6118						
	49782/GD	17	36.0700	<0.0001	18.0350	8.5626	154.4266			5.5158	18.7342	337.8716	
sna	50003/GD	32	3.0820	0.0791									
	50004/GD	33	0.1852	0.6670	2.1454	0.5810	1.2464			0.3121	6.6337	14.2319	
tor	6232/GD	31.5	3.1690	0.0751									
	101154/KK	31	2.5570	0.1098									
Predicting Power	36280/GD	31	0.5140	0.4734	1.5355	16.4688	25.2879			11.3850	16.3916	25.1693	
						1047.3007	17.2361	798.2716	875.2168	0.2913	0.2426		

Fly lifespan and motor behaviour are affected by *garz* knockdown in adult glia

As mentioned, we ranked the target genes from the RNAi confirmed predictions and decided to further investigate the top ranked target, *garz*, the fly orthologue for *GBF1*^{19,20,39}).

Pan-glial knockdown of *garz* with *repo-Gal4* specifically during adulthood strongly reduced lifespan. This was true for both RNAi lines tested when compared to *w¹¹¹⁸* median lifespan control (Figure 1B). Different glial cell types present in the adult fly brain have specific morphology and function⁴⁰. In order to test if a specific glial sub-population could account for the observed phenotype, we targeted the knockdown of *garz* using established Gal4 driver lines: astrocyte-like (*alrm-Gal4*), cortex (*NP2222-Gal4*), subperineural (*moody-Gal4*) and peripheral (*gliotactin-Gal4*) glia. In all sup-populations tested, the downregulation of *garz* caused a reduction in lifespan, albeit not as strong as the pan-glial knockdown (Figure 1C). This suggests that a combination of multiple functions is affected by *garz*.

We also analysed the effects of pan-neuronal (*elav-Gal4*) knockdown of *garz*. This also led to a significant shortening of lifespan although the effect was milder than the one obtained with pan-glial *garz* knockdown (Figure 1B vs 1C), either because of differences in Gal4 line strength or because of a higher impact of *garz* function in glial cells for maintenance of the brain homeostasis.

We then focused on rescuing the glia-related shorter lifespan phenotype using exogenous transgenes for *garz* and human *GBF1*. Although the overexpression of *garz* alone in adult glia had a very toxic effect, when combined with the *garz*-RNAi overexpression, promoted a modest but significant rescue of the lifespan (Figure 1D). This suggests that *garz* levels need to be tightly controlled in the fly. On the other hand, overexpression of the human *GBF1* was entirely neutral for fly lifespan when expressed on its own and fully rescued the lifespan phenotype when co-expressed with *garz* RNAi. This indicates a remarkable conservation in functions between *garz* and *GBF1*.

For both *garz* and *GBF1*, the presence of a functional Sec7 domain, which is responsible for the catalytic activity of GEF proteins domain²⁴, was important to exercise their rescue activity (Figure 1D). In the case of *UAS-garz*, a mutation of the Sec7 domain entirely eliminated the rescue of *garz* knock down, actually aggravating toxicity. This also indicates that the toxicity of *garz* overexpression is not dependent on the catalytic GEF function of *garz*, possibly suggesting a dominant negative effect by sequestration of binding partners in catalytically inactive complexes. Additionally, in the case of *UAS-GBF1*, the rescue effect was significantly reduced, albeit not entirely eliminated, by an inactive Sec7 domain (Figure 1D).

Human *GBF1* showed a remarkable capability to fully rescue lifespan shortening upon *garz* knockdown in glia. We then asked whether it would also be able to rescue the lifespan shortening induced by miRNAs predicted to target *garz*. From

our database analysis, miR-1, miR-79 and miR-315, all causing a strong reduction of lifespan¹¹, were among the miRNAs predicted to target *garz* and may be rescued by *GBF1*. Indeed, *UAS-GBF1* was able to significantly rescue the phenotypes caused by the overexpression of these miRNAs in glia (Figure 1E). *GBF1* co-overexpression was able to rescue the lifespan for miR-79 and miR-315 to what would be commonly observed in wild-type flies. These results confirm our initial predictions and establish *garz* as the main mediator of the effect on lifespan caused by overexpression of miR-79 and miR-315 in adult glia. The partial rescue of the miR-1 phenotype indicates that *garz* is only partially responsible for the effect of miR-1 in adult glia and is in accordance with the previously reported role of *repo* in miR-1-mediated lifespan shortening¹¹.

We have previously described an automated unbiased and high-throughput method to analyse fly motor activity¹¹). When using this paradigm, we unravelled an impact of glial *garz* knockdown on the amplitude of the response to a train of stimuli and *GBF1* co-overexpression rescued this response (Figure 2A). When looking at spontaneous activity parameters, i.e. non-stimulus driven, in the same experiment, flies expressing *garz*-RNAi showed a reduced average speed and an increased interval between bouts of movement without reflecting in the overall bout movement duration. Both average speed and inter-bout interval were fully rescued by the co-overexpression of *GBF1* (Figure 2B–D). This analysis indicates that *garz* knock down affects not only lifespan but also the healthspan and motor activity both exogenously stimulated and internally generated, making flies slower and also pausing more.

Subcellular effects of *garz* knockdown in adult glia

We next set out to determine the effects *garz* knock down had inside the glial cells that would correlate with behavioural and lifespan dysfunctions.

It has been reported that *garz* knockdown impairs vesicle transport and membrane delivery during fly development²⁵. Thus, we analysed membrane distribution in the presence of *garz*-RNAi in adult brains. Driving the expression *CD8-GFP* in glia showed aberrant membrane distribution upon *garz* knockdown when compared to a more homogeneous distribution of the GFP signal in glia from control brains (Figure 3A, Videos 1 and 2). Such data suggests that overall membrane trafficking in glia may be impaired although we have not been able to detect failure in membrane delivery of the cell adhesion cadherin molecule CadN (data not shown, the full dataset can be accessed at DOI 10.17605/OSF.IO/7HRZS).

Video 1. CD8-GFP in control brains. 3D reconstruction of confocal stacks imaging of panglial (*repo-Gal4*) CD8-GFP expression in a control brain. Note the smooth appearance of the glial membranes highlighted by the green signal. The full dataset can be accessed at DOI 10.17605/OSF.IO/96TS3.

1 video file

<https://doi.org/10.6084/m9.figshare.12162351.v1>⁴¹

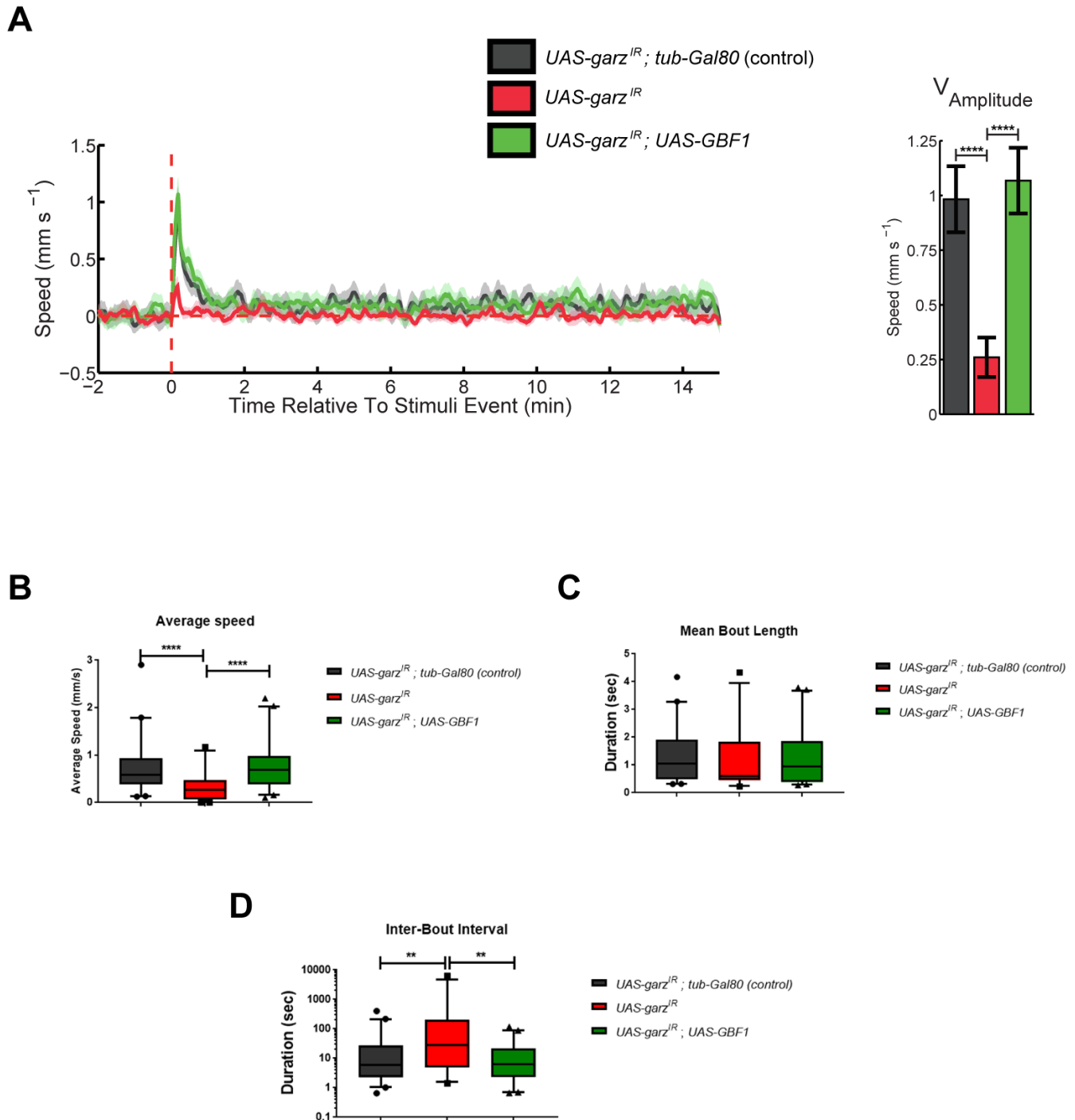


Figure 2. Knock down of *garz* in adult glial cells leads to significant impairment of fly motor functions. All data in this figure represent a grouping of two independent experiments with a total number of flies analysed (N) of 35–40. Error bars represent SEM in all graphs. Untreated track data can be accessed at DOI [10.17605/OSF.IO/UNJX7](https://doi.org/10.17605/OSF.IO/UNJX7). **(A)** Stimulus response curve for control flies (black), *garz* RNAi (red) and co-expression of GBF1 and *garz* RNAi (green). The graph is an average of 6 tracks for each of the stimuli received at 15 min intervals (See Methods). All genotypes also include *repo-Gal4* and *ubi-Gal80^{ts}* to express the transgenes in all adult glia. In control flies the presence of *tub-Gal80* blocks any expression of UAS-transgenes. The graph to the right reports the mean amplitude of the response to a train of stimuli, which is significantly reduced by RNAi against *garz*, and this reduction is reverted to normal level by co-expression of human GBF1. One-way ANOVA, Dunnett's multiple comparisons post hoc test. **(B)** Average speed analysis of the same flies as in A. RNAi against *garz* significantly slows down fly motility and this is rescued by human GBF1. One-way ANOVA, Dunnett's multiple comparisons post hoc test. **(C)** Mean bout length analysis of the same flies as in A. No significant difference is detected in this parameter. One-way ANOVA, Dunnett's multiple comparisons post hoc test. **(D)** Mean interbout interval analysis of the same flies as in A. RNAi against *garz* significantly increases the time spent in inactivity by flies and this is rescued by human GBF1. One-way ANOVA, Dunnett's multiple comparisons post hoc test.

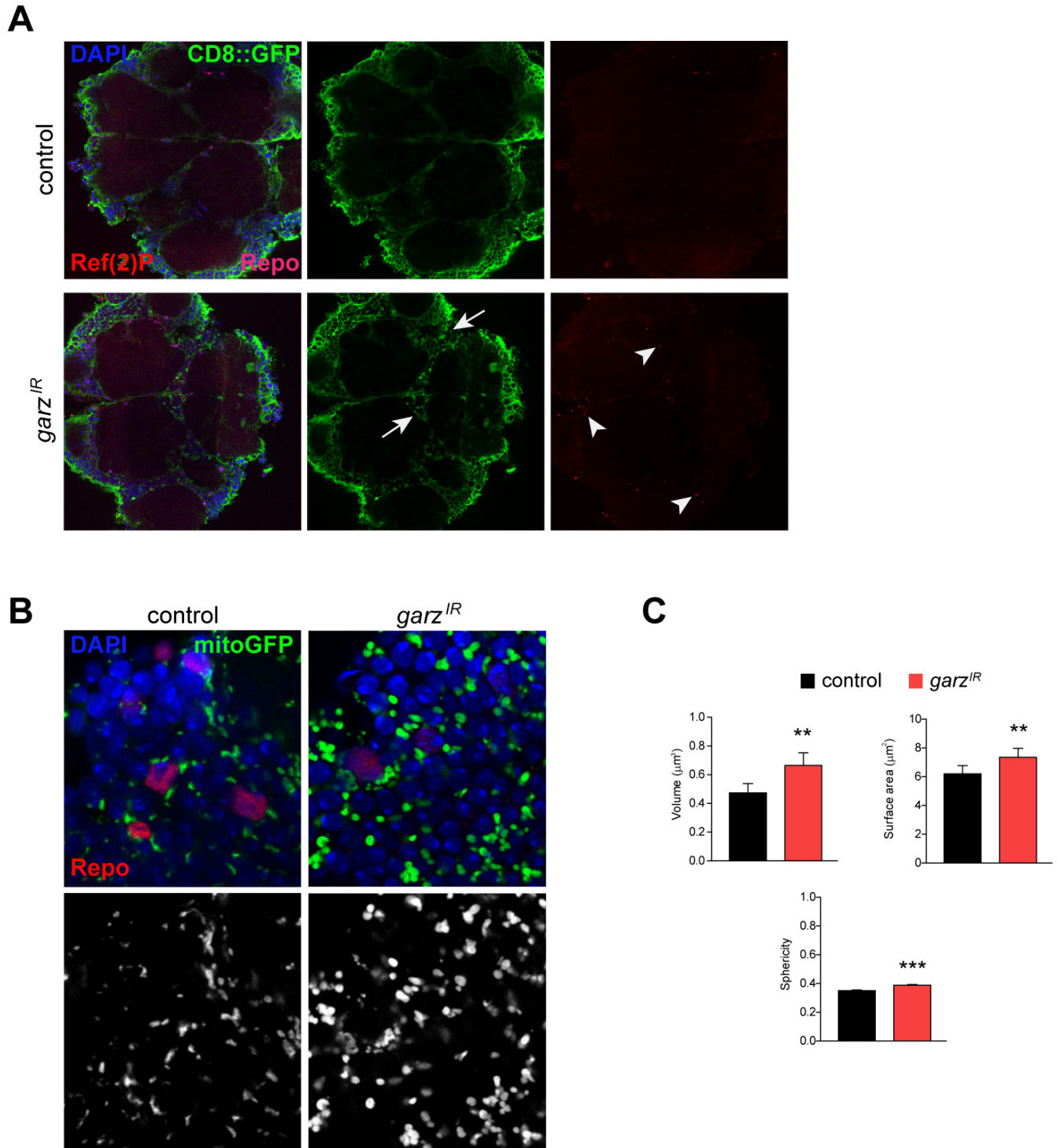


Figure 3. Sub-cellular dysfunctions caused by *garz* knock-down in adult glial cell. (A) Representative single confocal sections of adult fly brains stained for DAPI (blue), GFP (green), Repo (magenta) and Ref (2)P (red). Pan glial knock-down of *garz* with *repo-Gal4* and *ubi-Gal80^{ts}* leads to abnormal distribution of the plasma membrane targeted CD8-GFP protein (expressed from a *UAS-CD8-GFP* transgene in all glial cells) leading to gaps and blebs (arrows, see also Video1 and 2), and to accumulation of Ref(2)P puncta (arrowheads). The full dataset can be accessed at DOI [10.17605/OSF.IO/96TS3](https://doi.org/10.17605/OSF.IO/96TS3). (B) Representative single confocal section of adult fly brains stained for DAPI (blue), GFP (green) and Repo (red). The GFP signal also in back and white (lower panels) is due to the presence of a *UAS-mitoGFP* transgene and detects mitochondria. (C) Quantification of mitochondria parameters based on the GFP signal in B. Pan glial knock-down of *garz* with *repo-Gal4* and *ubi-Gal80^{ts}* leads to significant increases in the volume, surface area and sphericity of mitochondria. Mann-Whitney non-parametric test. N=300 objects, randomly selected from 4 brains. Error bars represent SEM. The full dataset can be accessed at DOI [10.17605/OSF.IO/EXMTG](https://doi.org/10.17605/OSF.IO/EXMTG).

Video 2. CD8-GFP in garz knock-down brains. 3D reconstruction of confocal stacks imaging of panglial (*repo-Gal4*) CD8-GFP expression in a *garz* knock-down brain. Note the clustering and blebs formed by the glial membranes highlighted by the green signal. The full dataset can be accessed at DOI [10.17605/OSF.IO/96TS3](https://doi.org/10.17605/OSF.IO/96TS3).

1 video file

<https://doi.org/10.6084/m9.figshare.12162393.v142>

Conflicting *in vitro* data has been reported for the effects of GBF1³¹ and *garz*³² in what concerns autophagy regulation. Looking at the distribution of the Ref(2)p (the orthologue of mammalian p62) autophagy receptor⁴³ revealed Ref(2)p accumulation in puncta, suggesting a potential block in autophagic clearance in glial cells (Figure 3A).

Finally, it has been suggested a role for GBF1 in the regulation of mitochondria morphology and function in yeast, *C. elegans* muscle and HeLa cells³⁰. Using *mito-GFP* transgene we were able to identify mitochondrial morphology defects in adult glial cells (Figure 3B, C). Quantification of the main morphological parameters has unravelled an overall increased mitochondrial volume, surface and sphericity upon *garz* knockdown. These parameters may indicate a defect in mitochondria quality control and are in agreement with an impaired autophagic clearance, which has the potential to also affect mitophagy.

Underlying data contains the raw data behind these results⁴⁴.

Discussion

We have previously screened a library of miRNAs for effects on *Drosophila*'s lifespan when expressed in adult glia and already established that this strategy can identify factors important for nervous system health in adult life¹¹. We aimed here at developing a generalizable global approach that would allow to identify the key target genes that mediate the actions of miRNAs in a given context. Focusing on miRNAs that shortened the lifespan, we devised an *in-silico* strategy to unravel a potential list of genes relevant for glial function and consequently brain homeostasis in adult flies. The outcome of this strategy had efficiency issues and highlighted the little overlap in the predictions made on the basis of four different databases for miRNA target prediction in *Drosophila*.

To put to the test the outcome of these *in silico* predictions⁴⁴, we have silenced individual genes by inducing the expression of specific RNAi in adult glia. The assumption being that RNAi downregulation of the top target genes would phenocopy the effect observed when expressing the miRNAs targeting them, i.e. lifespan reduction. Overall, however, the number of genes that, upon knockdown, reduced lifespan was remarkably low, and we could observe no tangible benefit of focusing on predictions in common to all four databases, versus targets differentially predicted in the different databases. It was also evident from our analysis that, among the databases, TargetScan and miRNA.org were considerably more efficient in delivering predictions that withstood the RNAi tests.

Therefore, the benefits of using miRNAs-based screens and *in silico* identification of targets, in place of much larger screens based on targeting single genes, have to be carefully evaluated and *in silico* selection of target genes should be based primarily on the TargetScan and miRNA.org databases. Nevertheless, the fraction of validated positive target genes by two criteria (7/65) and by at least one (22/65) is much larger than what usually expected in siRNA screens and suggests a 3/5-fold enrichment in positive hits. Thus, our method makes *Drosophila* screens a more appealing platform with reduced workload in comparison to traditional single gene targeted screens, whether by RNAi or genomic mutagenesis. This may have 3Rs benefits, facilitating the use of *Drosophila* as a model for preliminary studies on the genetic factors that influence a given biomedical process.

Our screen has also highlighted a number of genes that are strong, and in most cases unexpected, candidates for essential functions in adult glia in ageing. This list of genes provides a useful tool for scientists studying glial functions in ageing. In particular, all identified genes that have been validated by two RNAi lines have clear mammalian orthologues. *Drosophila* can therefore be used to study in detail the functions of these genes in the adult glial cells, in place of genetically modified mouse models.

To validate our findings, we focused on the top target of the genes commonly predicted by all databases and also by TargetScan, i.e. *garz*, the fly orthologue of the human GBF1.

The analysis of *garz* confirmed that this gene is absolutely required in adult glia, and also in neurons, for fly survival. Using our automated behavioural set up we could also establish that *garz* is essential in glia for locomotor activity in response to a stimulus or endogenously generated. Analysing the effects of silencing *garz* in different glial sub-populations showed that the strong reduction in lifespan could not be accounted for by one specific type of glia but rather due to a combined effect of silencing *garz* in all glial cells simultaneously, indicating that *garz* is essential for any glial cell type.

Our subcellular analysis suggests that the locomotor and lifespan defects correlate and possibly originate from a number of cellular defects in protein trafficking, autophagy and mitochondria quality control.

In *Drosophila*, mutated versions or knockdown of *garz* resulted in developmental epithelial morphogenesis defects^{20,21} and impaired membrane delivery of adhesion molecules²⁵. We have been able to identify membrane defects in glial membrane distribution, although not all membrane proteins seemed to be affected by *garz* knockdown.

garz and *GBF1* have been identified as a positive autophagy regulator in *Drosophila* primary cultured muscle cells³² and mammalian cells³¹. An accumulation of Ref(2)P upon *garz*-RNAi expression in adult glia suggests an autophagic clearance deficits, in agreement with these studies.

GBF1-RNAi has been shown to affect mitochondrial morphology and function³⁰. Chemical inhibition of GBF1 in mammalian cells also showed condensed mitochondria and mislocalisation in the cell⁴⁵. Although mislocalisation of mitochondria is difficult to assess due to glial cell morphology in the *Drosophila* brain, *garz*-RNAi strongly affected mitochondria morphology suggesting a more condensed state which may be a reflection of an unbalanced fission/fusion regulation and mitochondria quality control⁴⁶.

Our analysis further suggested that there was remarkable functional conservation between *garz* and human GBF1, with the latter being able to fully rescue, partially in a Sec7-domain dependent manner, the shorter lifespan and motor behaviour phenotypes caused by the silencing of *garz*. GBF1 was also able to rescue the lifespan shortening by three different miRNAs, miR-1, miR-79 and miR-315, validating that in our screen their effect is at least partially, and in some cases almost entirely, due to downregulation of *garz*.

Thus, these data validate both the logic and principles of miRNA screens, despite inefficiencies, and the use of *Drosophila* as a valid organism to study the biology of *garz/GBF1*.

The identification of major cellular events regulated by *garz/GBF1*^{27–29,47–49} has targeted such molecules for health and disease studies¹⁸. Recently, it has been shown that siRNA knock-down of GBF1 causes intracellular APP accumulation in primary cortical neurons; overexpression of GBF1 contributes to APP trafficking and is dependent on its GEF activity⁵⁰. Inhibition of GBF1 with brefeldin A was also shown to lead to a new form of cellular degeneration and death in neurodegenerative diseases, based on destruction of the nuclear lamina⁵¹.

Gbf1 conditional mutant mice have been generated in the Wellcome Trust Sanger Institute and are being phenotyped by the International Mouse Phenotyping Consortium (<https://www.mousephenotype.org/data/genes/MGI:1861607>). We demonstrate here that *Drosophila* would constitute an ideal organism to put forward 3Rs-compliant alternatives and, at least partially, replace this mouse line in studies aiming at understanding the role of GBF1 in health and disease.

Data availability

Underlying data

Open Science Framework: miRNA-garz. <https://doi.org/10.17605/OSF.IO/ASZST44>.

This project contains the following underlying data:

- **Table 2** (XLSX). (The complete **Table 2**.)
- **Table 2** Data – Pimental *et al.*, 2020 (XLSX). (Data underlying **Table 2**.)
- **Table 3** Data – Pimental *et al.*, 2020 (XLSX). (Data underlying **Table 3**.)

- **Table 4** Data – Pimental *et al.*, 2020 (XLSX). (Data underlying **Table 4**.)
- **Figure 1C** Data - Pimental *et al.*, 2020 (XLSX). (Data underlying **Figure 1C**.)
- **Figure 1D** Data - Pimental *et al.*, 2020 (XLSX). (Data underlying **Figure 1D**.)
- **Figure 1E** Data - Pimental *et al.*, 2020 (XLSX). (Data underlying **Figure 1E**.)
- **Figure 2** Data - Pimental *et al.*, 2020 (XLSX). (Data underlying **Figure 2**.)
- **Figure 3A** and videos. (TIFF images and ZIP files containing data underlying **Figure 3A**.)
- **Figure 3B-C**. (ZIP files containing raw images underlying **Figure 3B, C**.)
- **Extended data Table 1**- Data - Pimental *et al.*, 2020 (XLSX). (Data underlying **Extended data Table 1**.)
- **Extended data Table 2**- Data - Pimental *et al.*, 2020 (XLSX). (Data underlying **Extended data Table 2**.)
- **Extended data Table 3**- Data - Pimental *et al.*, 2020 (XLSX). (Data underlying **Extended data Table 3**.)
- **Extended data Table 4**- Data - Pimental *et al.*, 2020 (XLSX). (Data underlying **Extended data Table 4**.)
- Data not shown. (ZIP files containing images of membrane delivery of the cell adhesion cadherin molecule CadN.)

Extended data

Open Science Framework: miRNA-garz. <https://doi.org/10.17605/OSF.IO/K5HW938>.

This project contains the following extended data:

- **Extended Data Table 1. MicroCosm target prediction and ranking tables.** For each miRNA, ranking of target prediction - column (Score)*Av(χ^2) - was made by multiplying the Average χ^2 obtained in the screen (from **Table 1**) by the Score predicted in the MicroCosm database. In the total table, all values from a given target, resulting from all miRNAs were summed in a final ranking value in column $\Sigma(\text{Score}) * \text{Av}(\chi^2)$. This table and the full dataset can be accessed at DOI [10.17605/OSF.IO/R3ZX9](https://doi.org/10.17605/OSF.IO/R3ZX9).
- **Extended data Table 2. PicTar target prediction and ranking tables.** For each miRNA, ranking of target prediction - column (Score)*Av(χ^2) - was made by multiplying the Average χ^2 obtained in the screen (from **Table 1**) by the Score predicted in the PicTar database. In the total table, all values from a given target, resulting from all miRNAs were summed in a final ranking value in column $\Sigma(\text{Score}) * \text{Av}(\chi^2)$. This table and the full dataset can be accessed at DOI [10.17605/OSF.IO/MDKHR](https://doi.org/10.17605/OSF.IO/MDKHR).

- **Extended data Table 3. miRNA.org target prediction and ranking tables.** For each miRNA, ranking of target prediction - column $(\text{Score}^2) \cdot \text{Av}(\chi^2)$ - was made by multiplying the Average χ^2 obtained in the screen (from Table 1) by the square value of Score predicted in the miRNA.org database. The square value was used in this case as the scoring system used by miRNA.org delivers negative values, differently from the other databases. In the total table, all values from a given target, resulting from all miRNAs were summed in a final ranking value in column $\Sigma(\text{Score}^2) \cdot \text{Av}(\chi^2)$. This table and the full dataset can be accessed at DOI 10.17605/OSF.IO/539J8.
- **Extended data Table 4. TargetScan target prediction and ranking tables.** The TargetScan database does not provide a scoring system for its predictions, rather a list of 8mer or 7mer sequences matched by the miRNA on the target and an information on the conservation of these sequences. We have attributed a numerical score to these sequences privileging the importance of 8mer vs 7mer and of conservation according to the scheme

described in the Methods section. For each miRNA, ranking of target prediction - column $(\text{Score}) \cdot \text{Av}(\chi^2)$ - was made by multiplying the Average χ^2 obtained in the screen (from Table 1, some values specifically generated averaging all miRNA grouped in a single family by TargetScan) by the Score obtained according to our above-mentioned scheme. In the total table, all values from a given target, resulting from all miRNAs were summed in a final ranking value in column $\Sigma(\text{Score}) \cdot \text{Av}(\chi^2)$. This table and the full dataset can be accessed at DOI 10.17605/OSF.IO/WD6ZR.

Data are available under the terms of the [Creative Commons Attribution 4.0 International license](#) (CC-BY 4.0).

Acknowledgments

We thank M. Freeman, E.C. Lai, R. Sousa-Nunes, J. Bateman, S. Luschnig, the VDRC, the DSHB and the BDSC for fly stocks and reagents.

References

- Somjen GG: **Nervenkitz: notes on the history of the concept of neuroglia.** *Glia*. 1988; 1(1): 2–9.
[PubMed Abstract](#) | [Publisher Full Text](#)
- Allen NJ, Lyons DA: **Glia as architects of central nervous system formation and function.** *Science*. 2018; 362(6411): 181–185.
[PubMed Abstract](#) | [Publisher Full Text](#) | [Free Full Text](#)
- García-Cáceres C, Quarta C, Varela L, et al.: **Astrocytic Insulin Signaling Couples Brain Glucose Uptake with Nutrient Availability.** *Cell*. 2016; 166(4): 867–880.
[PubMed Abstract](#) | [Publisher Full Text](#)
- López-Colomé AM, López E, Mendez-Flores OG, et al.: **Glutamate Receptor Stimulation Up-Regulates Glutamate Uptake in Human Muller Glia Cells.** *Neurochem Res*. 2016; 41(7): 1797–805.
[PubMed Abstract](#) | [Publisher Full Text](#)
- Chaturvedi R, Luan Z, Guo P, et al.: **Drosophila Vision Depends on Carcine Uptake by an Organic Cation Transporter.** *Cell Rep*. 2016; 14(9): 2076–2083.
[PubMed Abstract](#) | [Publisher Full Text](#) | [Free Full Text](#)
- Rae C, Hare N, Bubbs WA, et al.: **Inhibition of glutamine transport depletes glutamate and GABA neurotransmitter pools: further evidence for metabolic compartmentation.** *J Neurochem*. 2003; 85(2): 503–14.
[PubMed Abstract](#) | [Publisher Full Text](#)
- Talbot S, Foster SL, Woolf CJ: **Neuroimmunity: Physiology and Pathology.** *Annu Rev Immunol*. 2016; 34: 421–47.
[PubMed Abstract](#) | [Publisher Full Text](#)
- Freeman MR: **Drosophila Central Nervous System Glia.** *Cold Spring Harb Perspect Biol*. 2015; 7(11): pii: a020552.
[PubMed Abstract](#) | [Publisher Full Text](#) | [Free Full Text](#)
- Lyons DA, Talbot WS: **Glial cell development and function in zebrafish.** *Cold Spring Harb Perspect Biol*. 2014; 7(2): a020586.
[PubMed Abstract](#) | [Publisher Full Text](#) | [Free Full Text](#)
- Zuchero JB, Barres BA: **Glia in mammalian development and disease.** *Development*. 2015; 142(22): 3805–9.
[PubMed Abstract](#) | [Publisher Full Text](#) | [Free Full Text](#)
- Mazaud D, Kottler B, Gonçalves-Pimentel C, et al.: **Transcriptional Regulation of the Glutamate/GABA/Glutamine Cycle in Adult Glia Controls Motor Activity and Seizures in Drosophila.** *J Neurosci*. 2019; 39(27): 5269–5283.
[PubMed Abstract](#) | [Publisher Full Text](#) | [Free Full Text](#)
- Bhat S, Jones WD: **An accelerated miRNA-based screen implicates Atf-3 in Drosophila odorant receptor expression.** *Sci Rep*. 2016; 6: 20109.
[PubMed Abstract](#) | [Publisher Full Text](#) | [Free Full Text](#)
- Trébuchet G, Cattenoz PB, Zsámboki J, et al.: **The Repo Homeodomain Transcription Factor Suppresses Hematopoiesis in Drosophila and Preserves the Glial Fate.** *J Neurosci*. 2019; 39(2): 238–255.
[PubMed Abstract](#) | [Publisher Full Text](#) | [Free Full Text](#)
- Colicelli J: **Human RAS superfamily proteins and related GTPases.** *Sci STKE*. 2004; 2004(250): RE13.
[PubMed Abstract](#) | [Publisher Full Text](#) | [Free Full Text](#)
- Cherfils J, Zeghouf M: **Regulation of small GTPases by GEFs, GAPs, and GDIs.** *Physiol Rev*. 2013; 93(1): 269–309.
[PubMed Abstract](#) | [Publisher Full Text](#)
- Gomez-Navarro N, Miller EA: **COP-coated vesicles.** *Curr Biol*. 2016; 26(2): R54–7.
[PubMed Abstract](#) | [Publisher Full Text](#)
- Stalder D, Antony B: **Arf GTPase regulation through cascade mechanisms and positive feedback loops.** *FEBS Lett*. 2013; 587(13): 2028–35.
[PubMed Abstract](#) | [Publisher Full Text](#)
- D'Souza-Schorey C, Chavrier P: **ARF proteins: roles in membrane traffic and beyond.** *Nat Rev Mol Cell Biol*. 2006; 7(5): 347–58.
[PubMed Abstract](#) | [Publisher Full Text](#)
- Claude A, Zhao BP, Kuziemyky GE, et al.: **GBF1: A novel Golgi-associated BFA-resistant guanine nucleotide exchange factor that displays specificity for ADP-ribosylation factor 5.** *J Cell Biol*. 1999; 146(1): 71–84.
[PubMed Abstract](#) | [Publisher Full Text](#) | [Free Full Text](#)
- Armbruster K, Luschnig S: **The Drosophila Sec7 domain guanine nucleotide exchange factor protein Gartenzwerg localizes at the cis-Golgi and is essential for epithelial tube expansion.** *J Cell Sci*. 2012; 125(Pt 5): 1318–28.
[PubMed Abstract](#) | [Publisher Full Text](#)
- Wang S, Meyer H, Ochoa-Espinosa A, et al.: **GBF1 (Gartenzwerg)-dependent secretion is required for Drosophila tubulogenesis.** *J Cell Sci*. 2012; 125(Pt 2): 461–72.
[PubMed Abstract](#) | [Publisher Full Text](#)
- Sáenz JB, Sun WJ, Chang JW, et al.: **Golginic A reveals essential roles for GBF1 in Golgi assembly and function.** *Nat Chem Biol*. 2009; 5(3): 157–165.
[PubMed Abstract](#) | [Publisher Full Text](#) | [Free Full Text](#)
- Zhao X, Claude A, Chun J, et al.: **GBF1, a cis-Golgi and VTCs-localized ARF-GEF, is implicated in ER-to-Golgi protein traffic.** *J Cell Sci*. 2006; 119(Pt 18): 3743–53.
[PubMed Abstract](#) | [Publisher Full Text](#)
- García-Mata R, Szul T, Alvarez C, et al.: **ADP-ribosylation factor/COP1-dependent events at the endoplasmic reticulum-Golgi interface are regulated by the guanine nucleotide exchange factor GBF1.** *Mol Biol Cell*. 2003; 14(6): 2250–61.
[PubMed Abstract](#) | [Publisher Full Text](#) | [Free Full Text](#)
- Szul T, Burgess J, Jeon M, et al.: **The Garz Sec7 domain guanine nucleotide exchange factor for Arf regulates salivary gland development in Drosophila.**

- Cell Logist.* 2011; 1(2): 69–76.
[PubMed Abstract](#) | [Publisher Full Text](#) | [Free Full Text](#)
26. Gupta GD, Swetha MG, Kumari S, *et al.*: **Analysis of endocytic pathways in *Drosophila* cells reveals a conserved role for GBF1 in internalization via GEECs.** *PLoS One.* 2009; 4(8): e6768.
[PubMed Abstract](#) | [Publisher Full Text](#) | [Free Full Text](#)
27. Zeng X, Han L, Singh SR, *et al.*: **Genome-wide RNAi screen identifies networks involved in intestinal stem cell regulation in *Drosophila*.** *Cell Rep.* 2015; 10(7): 1226–38.
[PubMed Abstract](#) | [Publisher Full Text](#) | [Free Full Text](#)
28. Morohashi Y, Balklava Z, Ball M, *et al.*: **Phosphorylation and membrane dissociation of the ARF exchange factor GBF1 in mitosis.** *Biochem J.* 2010; 427(3): 401–12.
[PubMed Abstract](#) | [Publisher Full Text](#)
29. Citterio C, Vichi A, Pacheco-Rodriguez G, *et al.*: **Unfolded protein response and cell death after depletion of brefeldin A-inhibited guanine nucleotide-exchange protein GBF1.** *Proc Natl Acad Sci U S A.* 2008; 105(8): 2877–82.
[PubMed Abstract](#) | [Publisher Full Text](#) | [Free Full Text](#)
30. Ackema KB, Hench J, Böckler S, *et al.*: **The small GTPase Arf1 modulates mitochondrial morphology and function.** *EMBO J.* 2014; 33(22): 2659–75.
[PubMed Abstract](#) | [Publisher Full Text](#) | [Free Full Text](#)
31. Naydenov NG, Harris G, Morales V, *et al.*: **Loss of a membrane trafficking protein α SNAP induces non-canonical autophagy in human epithelia.** *Cell Cycle.* 2012; 11(24): 4613–25.
[PubMed Abstract](#) | [Publisher Full Text](#) | [Free Full Text](#)
32. Zirin J, Nieuwenhuis J, Samsonova A, *et al.*: **Regulators of autophagosome formation in *Drosophila* muscles.** *PLoS Genet.* 2015; 11(2): e1005006.
[PubMed Abstract](#) | [Publisher Full Text](#) | [Free Full Text](#)
33. Lewis BP, Burge CB, Bartel DP: **Conserved seed pairing, often flanked by adenosines, indicates that thousands of human genes are microRNA targets.** *Cell.* 2005; 120(1): 15–20.
[PubMed Abstract](#) | [Publisher Full Text](#)
34. Bejarano F, Bortolamiol-Becet D, Dai Q, *et al.*: **A genome-wide transgenic resource for conditional expression of *Drosophila* microRNAs.** *Development.* 2012; 139(15): 2821–31.
[PubMed Abstract](#) | [Publisher Full Text](#) | [Free Full Text](#)
35. Nisoli I, Chauvin JP, Napoletano F, *et al.*: **Neurodegeneration by polyglutamine Atrophin is not rescued by induction of autophagy.** *Cell Death Differ.* 2010; 17(10): 1577–87.
[PubMed Abstract](#) | [Publisher Full Text](#)
36. Faville R, Kottler B, Goodhill GJ, *et al.*: **How deeply does your mutant sleep? Probing arousal to better understand sleep defects in *Drosophila*.** *Sci Rep.* 2015; 5: 8454.
[PubMed Abstract](#) | [Publisher Full Text](#) | [Free Full Text](#)
37. Bolte S, Cordeliers FP: **A guided tour into subcellular colocalization analysis in light microscopy.** *J Microsc.* 2006; 224(Pt 3): 213–32.
[PubMed Abstract](#) | [Publisher Full Text](#)
38. Fanto M: **miRNA-garz.** 2020.
<http://www.doi.org/10.17605/OSF.IO/K5HW9>
39. Pipaliya SV, Schlacht A, Klinger CM, *et al.*: **Ancient complement and lineage-specific evolution of the Sec7 ARF GEF proteins in eukaryotes.** *Mol Biol Cell.* 2019; 30(15): 1846–1863.
[PubMed Abstract](#) | [Publisher Full Text](#) | [Free Full Text](#)
40. Kremer MC, Jung C, Batelli S, *et al.*: **The glia of the adult *Drosophila* nervous system.** *Glia.* 2017; 65(4): 606–638.
[PubMed Abstract](#) | [Publisher Full Text](#) | [Free Full Text](#)
41. Fanto M: **Video 1. CD8-GFP in control brains.** 2020. f1000research.com. Media.
<http://www.doi.org/10.6084/m9.figshare.12162351.v1>
42. Fanto M: **Video 2. CD8-GFP in garz knock-down brains.** 2020. f1000research.com. Media.
<http://www.doi.org/10.6084/m9.figshare.12162393.v1>
43. Nezis IP, Simonsen A, Sagona AP, *et al.*: **Ref(2)P, the *Drosophila melanogaster* homologue of mammalian p62, is required for the formation of protein aggregates in adult brain.** *J Cell Biol.* 2008; 180(6): 1065–71.
[PubMed Abstract](#) | [Publisher Full Text](#) | [Free Full Text](#)
44. Fanto M: **Fork of miRNA-garz.** 2020.
<http://www.doi.org/10.17605/OSF.IO/A5ZST>
45. Walch L, Pellier E, Leng W, *et al.*: **GBF1 and Arf1 interact with Miro and regulate mitochondrial positioning within cells.** *Sci Rep.* 2018; 8(1): 17121.
[PubMed Abstract](#) | [Publisher Full Text](#) | [Free Full Text](#)
46. Pernas L, Scorrano L: **Mito-Morphosis: Mitochondrial Fusion, Fission, and Cristae Remodeling as Key Mediators of Cellular Function.** *Annu Rev Physiol.* 2016; 78: 505–31.
[PubMed Abstract](#) | [Publisher Full Text](#)
47. Martinez JL, Arnoldi F, Schraner EM, *et al.*: **The Guanine Nucleotide Exchange Factor GBF1 Participates in Rotavirus Replication.** *J Virol.* 2019; 93(19): e01062–19.
[PubMed Abstract](#) | [Publisher Full Text](#) | [Free Full Text](#)
48. Viktorova EG, Gabaglio S, Meissner JM, *et al.*: **A Redundant Mechanism of Recruitment Underlies the Remarkable Plasticity of the Requirement of Poliovirus Replication for the Cellular ArfGEF GBF1.** *J Virol.* 2019; 93(21): e00856–19.
[PubMed Abstract](#) | [Publisher Full Text](#) | [Free Full Text](#)
49. Ferlin J, Farhat R, Belouzard S, *et al.*: **Investigation of the role of GBF1 in the replication of positive-sense single-stranded RNA viruses.** *J Gen Virol.* 2018; 99(8): 1086–1096.
[PubMed Abstract](#) | [Publisher Full Text](#)
50. Liu K, Liu Y, Xu Y, *et al.*: **Regulatory role of Golgi brefeldin A resistance factor-1 in amyloid precursor protein trafficking, cleavage and A β formation.** *J Cell Biochem.* 2019; 120(9): 15604–15615.
[PubMed Abstract](#) | [Publisher Full Text](#)
51. Baron O, Boudi A, Dias C, *et al.*: **Stall in Canonical Autophagy-Lysosome Pathways Prompts Nucleophagy-Based Nuclear Breakdown in Neurodegeneration.** *Curr Biol.* 2017; 27(23): 3626–3642.e6.
[PubMed Abstract](#) | [Publisher Full Text](#) | [Free Full Text](#)

Open Peer Review

Current Peer Review Status:  

Version 1

Reviewer Report 22 June 2020

<https://doi.org/10.5256/f1000research.25558.r63653>

© 2020 Barclay J. This is an open access peer review report distributed under the terms of the [Creative Commons Attribution License](#), which permits unrestricted use, distribution, and reproduction in any medium, provided the original work is properly cited.



Jeff W. Barclay

Department of Cellular and Molecular Physiology, Institute of Translational Medicine, University of Liverpool, Liverpool, UK

This manuscript uses *Drosophila* to screen by miRNAs for essential glial genes, identifying and briefly investigating one of the candidates (*gartenzweg* or *garz*). The screen appears to be conducted well, the data logically presented and the outcomes interesting and novel. The screening method and methodological algorithm is straight-forward and described well. I have no negative issues with the experiments and believe this is a valid topic for publication that will prove useful to the community. In addition, I agree whole-heartedly that the 3Rs benefits are well demonstrated for studying miRNAs, glia and GBF1 biology specifically.

I have only minor suggestions for improvement, where the authors may want to reconsider wording to accurately reflect outcomes.

1. The overall interpretations of the manuscript are that this screen is identifying glial functions. From the manuscript, however, it is not clear what these functions actually are? The experiments manipulate expression in glial cells – and then measure broad outcome phenotypes such as lifespan and locomotion. However, I don't think the authors are necessarily suggesting that the function of glia is lifespan or locomotion. Later there are experiments that infer potential alterations to intracellular trafficking in glia, but I find these experiments more representative of *garz* function in glia rather than glial function itself.
2. The glia are targeted by miRNA expression and RNAi in the glia themselves. As miRNAs can be potentially released by exocytosis, it would be worthwhile to discuss the possibility for effects originating in other cells. The authors have done a nice control with the RNAi in neurons; however, this has partially replicated the glial RNAi effects and thus overall may reflect some transcellular effects.
3. The manuscript indicates remarkable conservation in function between *garz* and GBF1; however, I would suggest tempering that conclusion given that they do have divergent effects (e.g. one is toxic, one is not).

4. It isn't entirely clear why CD8 trafficking was selected for investigation over other possibilities. Given the lack of effect on cadherin trafficking, the speculation that overall trafficking in glia is impaired seems premature.

Are a suitable application and appropriate end-users identified?

Yes

If applicable, is the statistical analysis and its interpretation appropriate?

Yes

Are the 3Rs implications of the work described accurately?

Yes

Is the rationale for developing the new method (or application) clearly explained?

Yes

Is the description of the method technically sound?

Yes

Are sufficient details provided to allow replication of the method development and its use by others?

Yes

If any results are presented, are all the source data underlying the results available to ensure full reproducibility?

Yes

Are the conclusions about the method and its performance adequately supported by the findings presented in the article?

Yes

Competing Interests: No competing interests were disclosed.

Reviewer Expertise: Invertebrate models, genetics, neuroscience. Referee suggested by the NC3Rs for their scientific expertise and experience in assessing 3Rs impact.

I confirm that I have read this submission and believe that I have an appropriate level of expertise to confirm that it is of an acceptable scientific standard.

Reviewer Report 01 June 2020

<https://doi.org/10.5256/f1000research.25558.r62978>

© 2020 Bjedov I. This is an open access peer review report distributed under the terms of the [Creative Commons Attribution License](#), which permits unrestricted use, distribution, and reproduction in any medium, provided the original work is properly cited.



Ivana Bjedov

UCL Cancer Institute, University College London, London, UK

This manuscript by Gonçalves-Pimentel et al. describes an impressive series of very elegant and demanding longevity experiments used to develop an innovative methodological algorithm to identify and rank candidate genes that are targeted by miRNAs and that shorten lifespan when downregulated in adult glial cells. The work presented offers a comprehensive comparison of different miRNA target databases and link those to the longevity analysis screen. Advantage of miRNA is targeting multiple genes at once. For instance by screening 200 miRNA lines, this examines effect of down-regulation of approximately 6000 genes. However this subsequently presents a challenge to determine which genes are targeted with a particular miRNA and which gene is accountable for a given phenotype. Therefore, here, Gonçalves-Pimentel et al. produce an algorithm in which they link their miRNA lifespan screen results to multiple miRNA databases, with the final aim to rank genes that are predicted targets by these miRNA and that affect lifespan and ageing of the glial cells. Briefly, within each data base, each target score was multiplied by values of the lifespan screen results, and then ranking value for each target gene obtain for different data bases. Values obtained from all miRNA databases for each gene were summed for final ranking. This approach combined the effect of the miRNA on lifespan with the prediction of a gene being targeted by particular miRNA, using a variety of databases to strengthen the approach. Combining different databases is particularly important given a surprising difference in their target prediction.

The top candidate from the screen is a gene *garz*, (mammalian orthologue of GBF1), for which they predict that its down-regulation in the glia shorten lifespan. Advantage of such approach is that it offers possibility for screening in an invertebrate organism to uncover genes potentially important in mammalian glia.

garz is a target for three miRNA, *miRNA-1*, *miRNA-79*, and *miRNA-315*. The authors carefully examine its affect in different population of glial cells, replicate shorter lifespan using two different *garz* RNAi lines, overexpress human GBF1 to rescue short lifespan by these different miRNAs. Downregulation of *garz* in adult glial cells also leads to significant impairment of fly motor functions. The authors expanded their characterisation of *garz-RNAi* overexpressor flies further to show accumulation of Ref(2)P and likely consequent alterations/enlargement of mitochondria.

Overall this is a detailed and exhaustive study. The algorithm is clearly explained and well presented, and will certainly be useful in other miRNA studies and will inspire its adaptation to other miRNA screens. Moreover the authors developed a valuable list of genes that when down-regulated in glia impact lifespan. This is a really significant resource and dataset that the authors present and should be commended for. I only have a few minor points:

Were the longevity analysis done using males or females flies?

Why do the authors think that some of their predictions actually resulted in lifespan extension rather than shortening? Could the down-regulation of given gene have different outcomes when it occurs in concert with other miRNA gene target downregulation? Could this be commented in discussion perhaps?

How easily can their method be adapted for a different screen using a different output, such as for instance miRNA screen for stress resilience?

In the ageing field, lifespan extension is a gold standard to detect anti-ageing genes and interventions. Could the authors comment on finding genes that extend lifespan in glia rather than shorten it?

The authors say” Recently, it has been shown that siRNA knockdown of GBF1 causes intracellular APP accumulation in primary cortical neurons”, could they please define APP.

In Figure 1 and 2 driver names are not very visible, could this be improved for clarity or genotypes be written in full perhaps?

In Figure 3A, it is not very visible what the arrows is pointing at, at least not in my downloaded version of the article.

Overall, this is a very valuable resource for anyone working on miRNA and glial cell. This research is an excellent example how screens in invertebrate organisms can lead to discoveries of important biological functions of mammalian orthologues.

Are a suitable application and appropriate end-users identified?

Yes

If applicable, is the statistical analysis and its interpretation appropriate?

Yes

Are the 3Rs implications of the work described accurately?

Yes

Is the rationale for developing the new method (or application) clearly explained?

Yes

Is the description of the method technically sound?

Yes

Are sufficient details provided to allow replication of the method development and its use by others?

Yes

If any results are presented, are all the source data underlying the results available to ensure full reproducibility?

Yes

Are the conclusions about the method and its performance adequately supported by the findings presented in the article?

Yes

Competing Interests: No competing interests were disclosed.

Reviewer Expertise: ageing, mTOR, autophagy, Drosophila

I confirm that I have read this submission and believe that I have an appropriate level of expertise to confirm that it is of an acceptable scientific standard.

The benefits of publishing with F1000Research:

- Your article is published within days, with no editorial bias
- You can publish traditional articles, null/negative results, case reports, data notes and more
- The peer review process is transparent and collaborative
- Your article is indexed in PubMed after passing peer review
- Dedicated customer support at every stage

For pre-submission enquiries, contact research@f1000.com

F1000Research